Molecular Phylogenetics and Evolution 183 (2023) 107705

Contents lists available at ScienceDirect

Molecular Phylogenetics and Evolution

journal homepage: www.elsevier.com/locate/ympev

In the land of the blind: Exceptional subterranean speciation of cryptic troglobitic spiders of the genus *Tegenaria* (Araneae: Agelenidae) in Israel

Shlomi Aharon [a,b,*], Jesús A. Ballesteros [c], Guilherme Gainett [d], Dror Hawlena [b], Prashant P. Sharma [d], Efrat Gavish-Regev [a,*]

[a] The National Natural History Collections, The Hebrew University of Jerusalem, Edmond J. Safra Campus, Givat Ram, Jerusalem 9190401, Israel
[b] Department of Ecology, Evolution & Behavior, Edmond J. Safra Campus, Givat Ram, Jerusalem 9190401, Israel
[c] Department of Biology, Kean University, Union, NJ 07083, USA
[d] Department of Integrative Biology, University of Madison-Wisconsin, 441 Birge Hall, 430 Lincoln Drive, Madison, WI 53706, USA

ARTICLE INFO

Keywords:
Caves
Cryptic species
Funnel-web spiders
Levant
Microendemism
Troglomorphism

ABSTRACT

Caves have long been recognized as a window into the mechanisms of diversification and convergent evolution, due to the unique conditions of isolation and life in the dark. These lead to adaptations and reduce dispersal and gene flow, resulting in high levels of speciation and endemism. The Israeli cave arachnofauna remains poorly known, but likely represents a rich assemblage. In a recent survey, we found troglophilic funnel-web spiders of the genus *Tegenaria* in 26 caves, present mostly at the cave entrance ecological zone. In addition, we identified at least 14 caves inhabited by troglobitic *Tegenaria,* which are present mostly in the twilight and dark ecological zones. Ten of the caves, located in the north and center of Israel, are inhabited by both troglophilic and troglobitic *Tegenaria*. These spiders bear superficial phenotypic similarities but differ in the levels of eye reduction and pigmentation. To test whether these taxa constitute separate species, as well as understand their relationships to epigean counterparts, we conducted a broad geographic sampling of cave-dwelling *Tegenaria* in Israel and Palestine, using morphological and molecular evidence. Counterintuitively, our results show that the troglobitic *Tegenaria* we studied are distantly related to the troglophilic *Tegenaria* found at each of the cave entrances we sampled. Moreover, seven new troglobitic species can be identified based on genetic differences, eye reduction level, and features of the female and male genitalia. Our COI analysis suggest that the Israeli troglobitic *Tegenaria* species are more closely related to eastern-Mediterranean congeners than to the local sympatric troglophile *Tegenaria* species, suggesting a complex biogeographic history.

1. Introduction

Speciation is an intricate evolutionary process that is affected by biotic and abiotic variables. There are several non-mutually exclusive ecological and evolutionary mechanisms that can help elucidate a specific speciation event (Gavrilets, 2003; Schluter, 2009). Yet, finding the mechanisms of speciation requires a precise understanding of the degree of geographical and reproductive isolation between populations, as well as the history of the species distribution ranges (Gavrilets, 2014; Reznick and Ricklefs, 2009; Savolainen et al., 2006; Turelli et al., 2001). After divergence occurs, reproductive isolation is necessary for maintaining the divergent species, but other ecological and evolutionary processes can later mask this evolutionary scenario (Bolnick and Fitzpatrick, 2007; Rundle and Nosil, 2005).

Caves constitute promising arenas for investigating mechanisms of speciation, due to their isolation from surface habitats and unique suite of environmental conditions (Howarth, 1993; Mammola, 2019; Snowman et al., 2010). The degree of isolation of caves may lead to low dispersal and low gene flow between populations of cave-dwelling organisms (Tobin et al., 2013). Although caves can be found in different environments, they share many biotic and abiotic characteristics, such as narrow range of temperatures, high relative humidity, and limitation of light and nutrients (Poulson and White, 1969). These conditions may enhance both metabolic and morphological modifications, and may lead to selection for cave adaptations, resulting in high levels of speciation and endemism (Arnedo et al., 2007; Barr and Holsinger, 1985;

* Corresponding authors at: The National Natural History Collections, The Hebrew University of Jerusalem, Edmond J. Safra Campus, Givat Ram, Jerusalem 9190401, Israel (Shlomi Aharon and Efrat Gavish-Regev).
E-mail addresses: shlomi.aharon1@mail.huji.ac.il (S. Aharon), efrat.gavish-regev@mail.huji.ac.il (E. Gavish-Regev).

https://doi.org/10.1016/j.ympev.2023.107705
Received 24 August 2022; Received in revised form 14 December 2022; Accepted 11 January 2023
Available online 24 January 2023

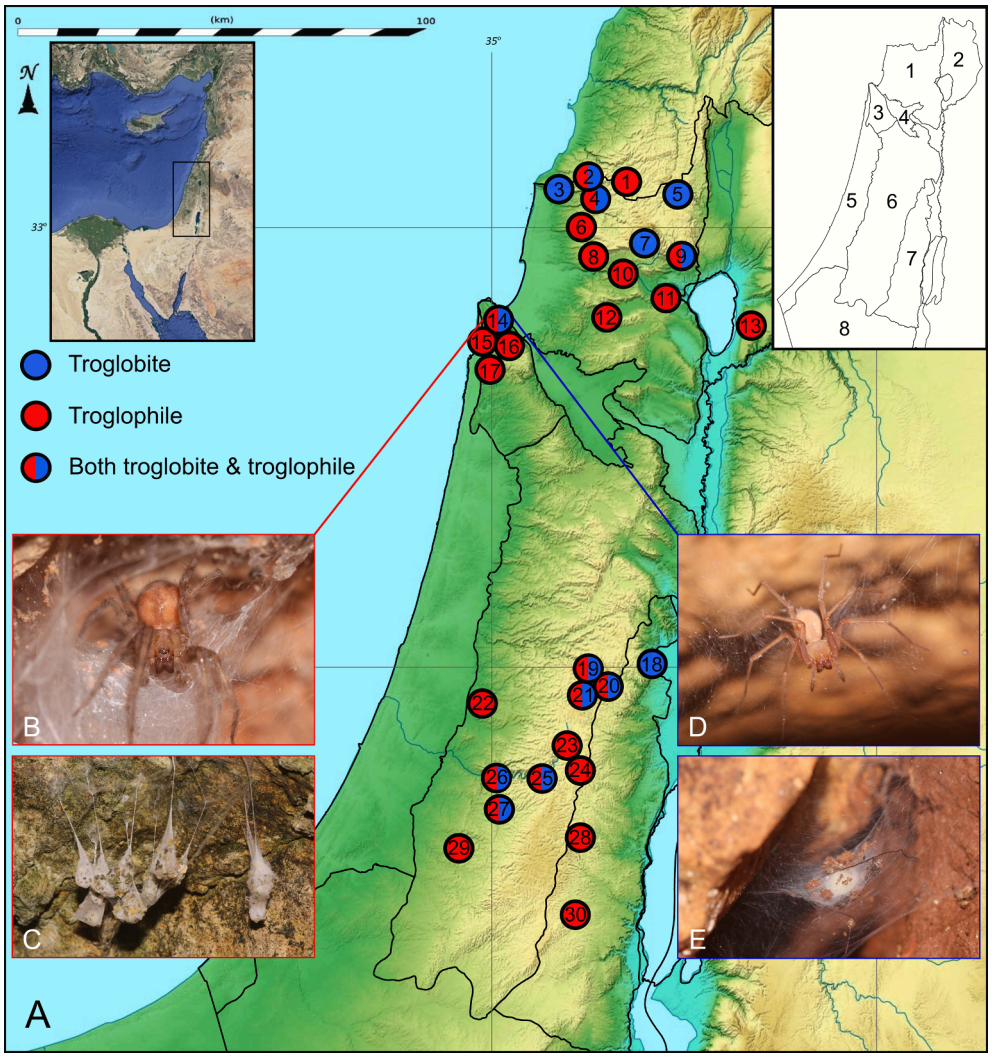

Fig. 1. Distribution of 30 caves inhabited by *Tegenaria* species. **A.** Map of Israel showing caves inhabited by troglobitic (blue dots), troglophilic (red dots), or both in the same cave (half blue and red dots). Numbers representing the caves correspond to Supplementary Table 1. **Right inset map** shows the geographical regions of Israel. 1. upper and lower Galilee. 2. Golan heights and Hula plain. 3. Karmel mountain and Menashe heights. 4. Yizre'el valley. 5. Coastal plain. 6. Judea and Samaria mountains. 7. Judean desert. 8. Negev desert. **B.** Eye bearing *Tegenaria pagana* from Ornit cave entrance (Fig. 1, #14). **C.** Egg sacs of *Tegenaria angustipalpis* hung from the cave ceiling (characteristic of troglophilic species), photographed at Beit-Jann cave entrance (Fig. 1, #7). **D.** Eyeless *Tegenaria ornit* sp. nov. from the dark zone of Ornit cave (Fig. 1, #14). **E.** Egg sac of *Tegenaria trogalil* sp. nov., oviposited in the middle of the sheet-web, in Hutat-Seter cave (Fig. 1, #9) and characteristic of troglobitic species. (For interpretation of the references to colour in this figure legend, the reader is referred to the web version of this article.)

Mammola, 2019; Mammola et al., 2018, 2015). The adaptations of troglobites can include regressive traits (e.g., the reduction or complete loss of eyes; depigmentation; loss of circadian rhythm; low metabolic rate) and constructive ones (e.g., elongation of appendages; compensatory increase of sensory organs; Howarth and Moldovan, 2018; Protas and Jeffery, 2012; Romero Díaz and Fenolio, 2009). As a result, hypogean habitats are unique ecosystems that harbor many exceptional organisms adapted to life in the dark, known as troglobites or obligate cave-dwelling species (Trajano, 2012; Trajano and de Carvalho, 2017).

Two major hypotheses were suggested to explain speciation in caves and the origin of obligate cave-dwelling species: the Adaptive Shifts Hypothesis (ASH) and the Climatic Relict Hypothesis (CRH). ASH postulates that animals colonize caves to exploit novel resources. These individuals experience divergent (ecological) selection in sympatry or parapatry to the source population (Howarth, 1987; Rivera et al., 2002). By contrast, CRH postulates that climatic changes that lead to extirpation of the epigean ancestor from the environment outside the cave left the relict cave-populations in complete geographic isolation, leading to allopatric speciation in those hypogean "islands" (Barr and Holsinger, 1985; Snowman et al., 2010). The two hypotheses are not mutually exclusive and a third scenario that combines both is also possible (e.g., active cave colonization followed by divergent selection, with subsequent extirpation of the epigean ancestor from the surface due to climatic events and aridification (Aharon et al., 2019; Juan et al., 2010)). Presently, most examples supporting ASH come from islands and from tropical or sub-tropical climates, whereas most examples supporting CRH are known from regions that were affected by glaciation events, mainly in the Palearctic (Arnedo et al., 2007; Howarth, 2019, 1980; Mammola et al., 2018, 2015).

Our goal was to untangle speciation mechanisms in light of historical climatic events in Levantine caves, a geographic region that was never covered by glaciers, but experienced dramatic climatic changes during the last 23.5 million years (Tchernov, 1988). In the study area, troglomorphic and eye-bearing morphotypes of funnel-web spiders (Agelenidae, *Tegenaria*) occur in close geographic proximity and are often found inhabiting the same cave. The close proximity of these congeneric populations, along with the superficial morphological similarities in somatic and reproductive anatomy, imply either several cave colonization events, and/or different divergence scenarios from a recent or an extinct ancestor species (Trontelj, 2018). We aimed to test how the troglomorphic and eye-bearing morphotypes found in different ecological zones of the caves are related, toward understanding the history of habitat colonization. We conducted a broad geographic sampling of *Tegenaria* inside and outside of 30 caves in Israel and Palestine. We inferred the evolutionary relationships of these spiders through a combination of morphological approaches, COI barcoding, and ddRAD sequencing.

Currently, 120 species are included in the genus *Tegenaria* Latreille, 1804 ("WSC. Ver. 23.5.," 2022), and of these 19 species are associated with epigean habitats but also reported as maintaining stable hypogean populations in Europe (i.e.; troglophile species), (Mammola et al., 2022a, 2022b). In Israel, *Tegenaria* was known by eight epigean species

(Levy, 1996), and until recently, there was not a single documentation of *Tegenaria* spiders from hypogean habitats. Following several excursions dedicated to cave arachnofauna, we found that four of the species known from Israel (namely *T. angustipalpis* Levy, 1996, *T. dalmatica* Kulczyński, 1906, *T.* cf. *epacris* Levy, 1996, and *T. pagana* C. L. Koch, 1840) are troglophiles (Cuff et al., 2021; Gavish-Regev et al., 2021). Additionally, we found seven obligatory cave-dwelling (troglobites) *Tegenaria* species, new to science, all of which are microendemics and have some level of troglomorphism. Here, we show that the Israeli troglobite *Tegenaria* species belong to a clade together with species of the *T. ariadnae* and *T. percuriosa* species complexes. This clade harbors deep species-level divergences and is distantly related to a clade that includes the widespread troglophile eye-bearing *Tegenaria* species inhabiting the epigean habitats and cave entrance in our system.

2. Material and methods

2.1. Species sampling

We studied ca. 200 individuals of the funnel-web genus *Tegenaria* newly collecting in more than ten designated field surveys between 2014 and 2022 (Gavish-Regev et al., 2021, 2016). During these surveys, we visited ca. 100 caves across Israel, of which 30 were inhabited by *Tegenaria* spiders (Fig. 1; Supplementary Table 1). Specimens were hand-collected while visually searching along the walls and between stones at four ecological zones: the cave entrance, the twilight zone, the dark zone and outside each cave near the cave entrance (see Gavish-Regev et al., 2021, 2016). Specimens were preserved in 75 % ethanol for morphological analyses or in 96 % ethanol for molecular analyses and are deposited at the National Natural History Collections (NNHC), The Hebrew University of Jerusalem (HUJ-INVAr). In addition, we examined ca. 30 individuals belonging to seven *Tegenaria* species, deposited in NNHC (HUJ-INVAr), that were previously revised by Gershom Levy (Levy, 1996). The research was conducted with collection permits 2013/40027, 2013/40085, 2014/40313, 2015/40992, 2017/41718, 2018/42037 2018/41999, 2020/42450, 2021/42815, and 2022/43117 from the Israel Nature and Parks Authority to Efrat Gavish-Regev. Transliterated names of the localities follow the "Toponomasticon. *Geographical gazetteer of Israel*" published by Survey of Israel (1994) and "Israel Touring Map" (1:250,000). Geographic coordinates are given in WGS84. The distribution map was generated using ArcGIS Online and Inkscape (ver. 0.92.4). Morphological descriptions and specimen lists were generated following Magalhaes (Magalhaes, 2019).

2.2. Morphological data collection

Morphological examination of the specimens was performed using a Nikon SMZ25 motorized stereomicroscope mounted with a Nikon DS-F12 camera, driven by NIS-Elements D v. 4.20 software (Nikon). Image stacks were combined using Zerene Stacker (Version 1.04) and edited using GIMP (ver. 2.10.10) and Inkscape (ver. 0.92.4). Left pedipalps were illustrated. For clearing the female genitalia, the removed epigynes were cleared using a 10 % KOH solution. All measurements are given in millimeters. Leg measurements were taken from the dorsal side, measurements of pedipalps and legs are given in the order of femur, patella, tibia, metatarsus, tarsus/cymbium. The morphological terminology follows Bolzern (Bolzern et al., 2013).

2.2.1. Abbreviations

AER, anterior eye row; ALE, anterior lateral eyes; ALS, anterolateral sclerite of median plate of epigynum; AME, anterior median eyes; C, conductor; CD, copulatory duct; CO, copulatory opening at female epigynum; DB, dorsal branch of retrolateral tibial apophysis; E, embolus; FD, fertilization duct; LB, lateral branch of retrolateral tibial apophysis; LM, lateral margin of epigynum; LVR, lateroventral ridge of retrolateral tibial apophysis; MA, median apophysis of male bulb; MP, median plate of epigynum; PER, posterior eye row; PLE, posterior lateral eyes; PME, posterior median eyes; PR, pale region of median plate; RC, receptaculum; RTA, retrolateral tibial apophysis; TEC, terminal end of conductor.

2.3. Molecular data analysis

To determine the relationships of Israeli cave-dwelling *Tegenaria* to each other as well as other congeners outside Israel, we used ddRAD sequencing (Elshire et al., 2011; Peterson et al., 2012) and COI (mitochondrial locus cytochrome *c* oxidase subunit I) barcoding of spiders representing 30 cave localities from Israel. The mitochondrial locus COI was included to enhance integration of data with legacy Sanger datasets.

2.3.1. Molecular sequencing and analysis of ddRAD

All samples used for ddRAD sequencing were collected during 2018. Specimens were directly preserved in the field in 96 % ethanol and stored at −20° C until processing. We selected 64 specimens (Supplementary Table 2) representing the breadth of geographic and phenotypic diversity for genome-wide restriction site associated sequencing, to inform phylogenetic structure from single nucleotide polymorphism (SNPs). Total DNA was extracted from legs and cephalothorax using the Qiagen DNEasy® Blood and Tissue extraction kit. The purity and concentration of extractions were verified by spectrophotometry using a Nanodrop ONE. A minimum 500 ng of genomic DNA was used for enzyme optimization, digestion, library preparation and sequencing at CD Genomics (additional details can be found at https://www.cd-genomics.com/ddrad-seq.html). Following optimization, samples were digested with the restriction enzymes *NsiI* and *BfaI* and paired end sequenced on an Illumina HiSeq2500 platform with 150 bp read lengths.

Raw reads of 58 out of the 64 specimens were processed with the ipyrad pipeline v. 0.9.68 (Eaton and Overcast, 2020) for demultiplexing, quality filtering, assembly and SNP discovery. Settings in the control file used ddRAD options, with phred quality score threshold < 33, a minimum 6X depth for base calling and 0.85 similarity threshold to cluster homologous RAD loci. Only loci present in a minimum of four samples were retained for downstream analyses. The output sequence files containing single nucleotide polymorphisms (SNPs) were used as the primary datasets for phylogenetic inference. To explore the effect of completeness/missing data, additional datasets were produced with trimAl v 1.4 (Capella-Gutierrez et al., 2009). Phylogenetic trees were estimated with IQTREE v 1.6.11 (maximum likelihood) using Model Finder and ultrafast bootstrap options (Hoang et al., 2018; Kalyaanamoorthy et al., 2017; Nguyen et al., 2015).

2.3.2. Sequencing and analysis of COI locus

Barcoding fragment of the cytochrome *c* oxidase subunit I (COI) mitochondrial gene was amplified for 60 out of the 64 specimens, collected by us, using LCO1409 and HCO2198 primer pair, and 2ul of the same genomic extractions was used for ddRAD as template. PCR reactions were carried out in 25ul reactions with AmpliTaq360 (Thermo Fisher), following the manufacturer's protocol. The PCR thermal profile consisted of initial denaturation for 3 mins at 95 °C, followed by 37 cycles of 30 s at 95 °C, 45 s at 47 °C and 1 min at 72 °C; and a final extension step of 7 mins at 72 °C. PCR products were purified with the Gene JET PCR® purification Kit (Thermo Fisher) and Sanger-sequenced following standard protocols at MacroGen (Maryland). Chromatograms were cleaned and assembled into contigs in Geneious v 11. 1.5. The barcoding dataset was enriched with publicly available sequences of 37 additional specimens, including other *Tegenaria* species as well as *Malthonica oceanica* Barrientos & Cardoso, 2007 and *Histopona torpida* (C. l. Koch, 1837) as the outgroups (Supplementary Table 3). Multiple sequence alignment was conducted in Mafft v 7.471 (Katoh and Standley, 2013) and inspected for open reading frame. Phylogenetic analyses in IQTREE (maximum likelihood) used the same options as above, with model testing (TIM3 + F + I + G4) and under a codon-specific model for

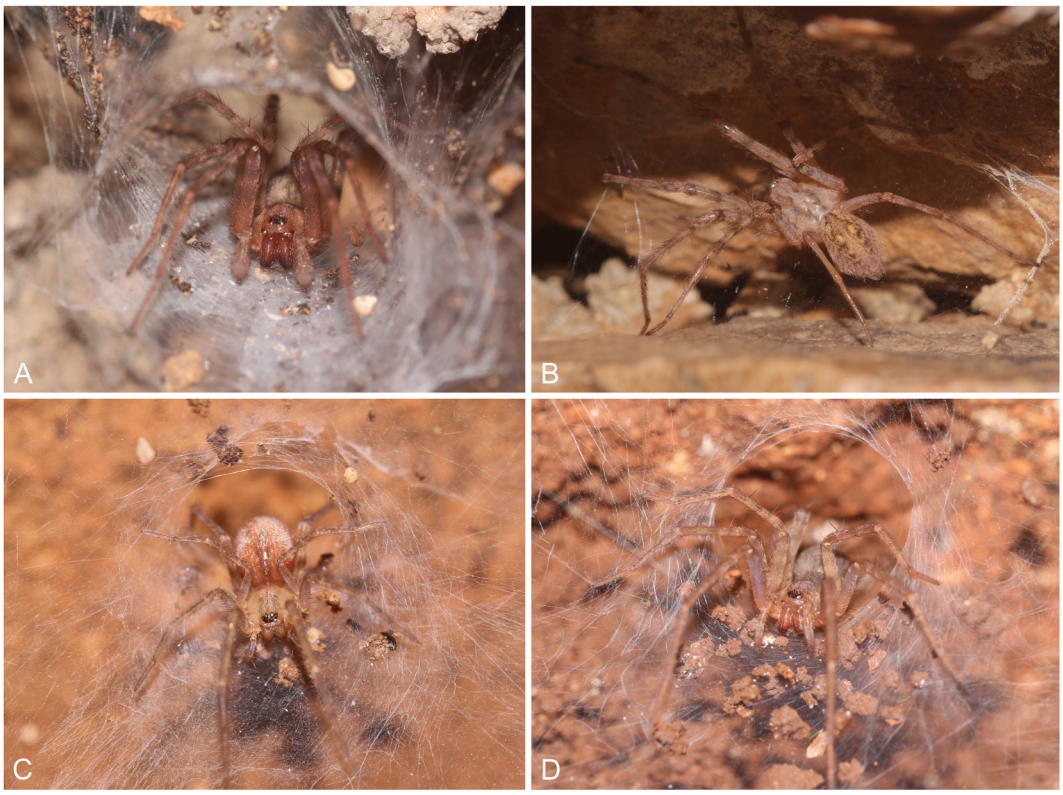

Fig. 2. Four troglophilic species found at cave entrances and twilight zones. **A.** *Tegenaria pagana* C. L. Koch, 1840. **B.** *Tegenaria dalmatica* Kulczyński, 1906. **C.** *Tegenaria* cf. *epacris* Levy, 1996. **D.** *Tegenaria* cf. *angustipalpis* Levy, 1996.

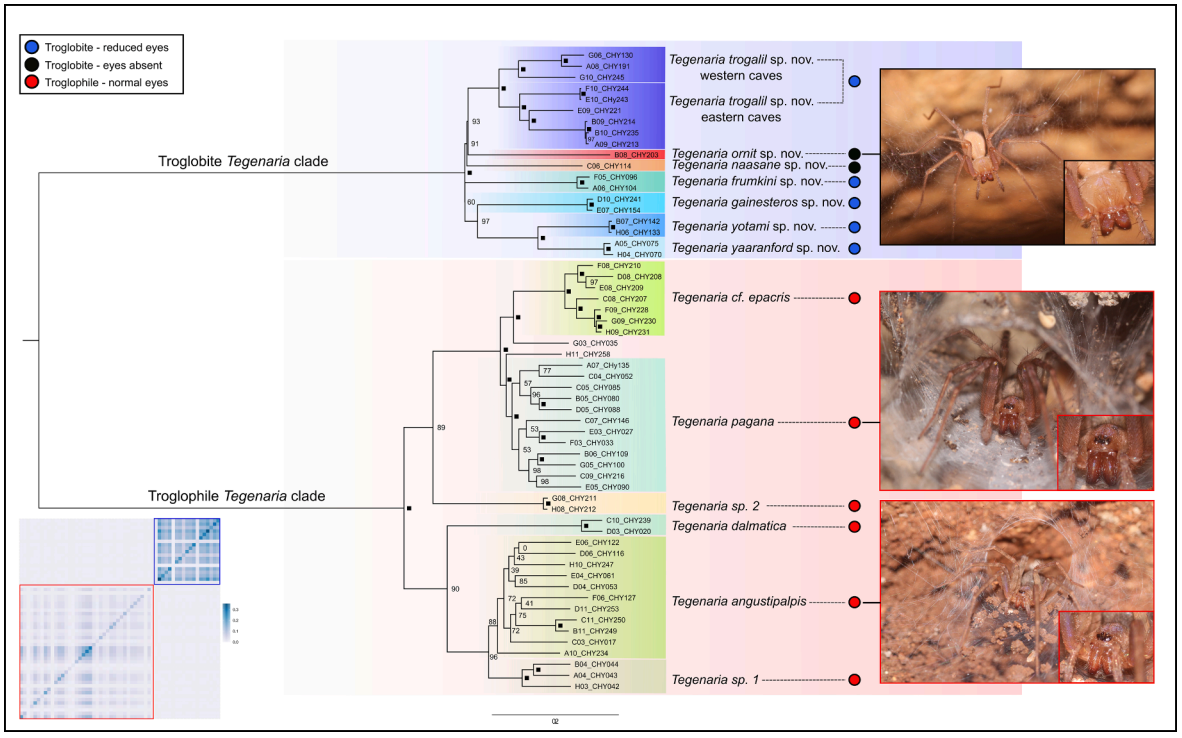

Fig. 3. Maximum likelihood tree topology of reduced eyes (blue dots) and eyeless (black dots) *Tegenaria* present at the deep sections of the caves and eye-bearing *Tegenaria* present at cave entrance (red dots), based on SNP dataset (50% taxon occupancy, trimmed dataset) represent bootstrap support. Black squares indicate fully supported clades. Upper picture: eyeless *Tegenaria ornit* sp. nov. from the dark chamber in Ornit cave; Middle picture: eye-bearing *Tegenaria pagana* from Te'omim cave twilight zone; Lower picture: eye-bearing *Tegenaria angustipalpis* from Shetula cave entrance. Inset: heatmap showing frequency of shared loci among 58 OUT's based on 382,027 loci inferred by ddRAD sequencing analysis using ipyrad. Note the different clusters of the reduced eyes *Tegenaria* at the top right and the eye-bearing species from the cave entrance. (For interpretation of the references to colour in this figure legend, the reader is referred to the web version of this article.)

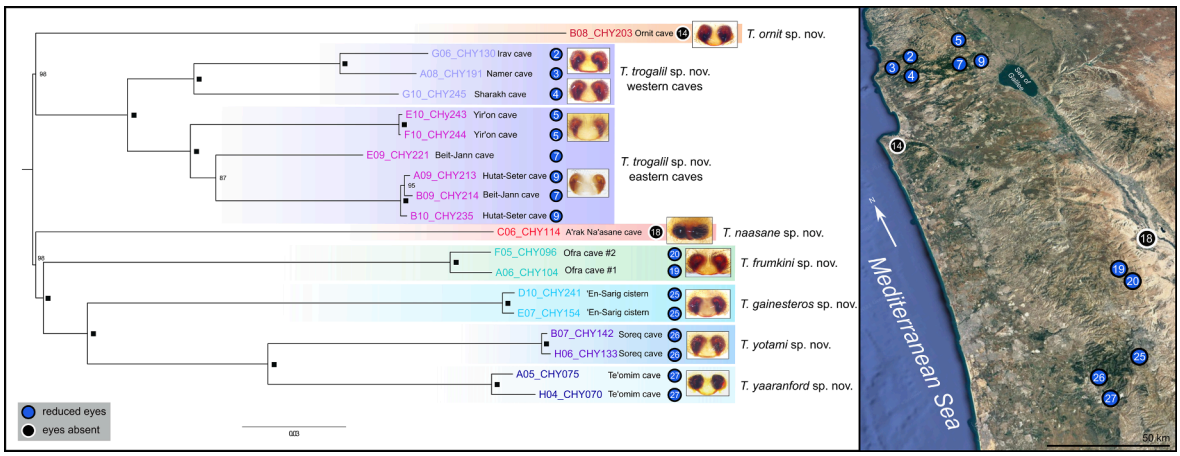

Fig. 4. Maximum likelihood tree topology of 19 samples of the troglobitic (eyeless and reduced eyes) *Tegenaria* present at the deep section of the caves, based on SNP dataset (25% missing data). Numbers at nodes represent bootstrap support. Black squares indicate fully supported clades. Caves with completely blind *Tegenaria* species Ornit (14) and A'rak Na'asane (18) appear as black circles on the map, while caves with reduced-eye *Tegenaria* species appear as blue circles on the map. (For interpretation of the references to colour in this figure legend, the reader is referred to the web version of this article.)

the invertebrate mitochondrial genetic code (Codon5). GenBank accession numbers are provided in Supplementary Tables 2-3.

Bayesian phylogenetic analyses and dating were conducted in Beast (v2.6.7) and associated packages (Bouckaert et al., 2019) with TN93 + I + G and Yule as the substitution and tree model, respectively, following model-testing (above). For dating, analyses were run using strict and relaxed (ucln) clock models, both with a fixed mean rate of 0.0115, following Bidegaray-Batista and Arnedo (Bidegaray-Batista and Arnedo, 2011). For both clock models, the analyses was run for 10 x10^6 iterations across four independent chains. Stationarity and convergence were assessed in Tracer (v1.7.2) (Rambaut et al., 2018) and sampled trees were combined after discarding 10 % as burnin to produce maximum credibility trees using TreeAnnotator (v2.6.6) (Rambaut et al., 2018).

3. Results

3.1. Biodiversity assessments

In 26 of the 30 caves where *Tegenaria* were found, we documented troglophilic species (species that have both hypogean and epigean populations in Israel) mostly at the cave entrance and twilight ecological zones. In 14 caves we found troglobitic species at the twilight and dark ecological zones. In ten caves we found both troglophilic and troglobitic *Tegenaria*, sometimes even sharing the same location within the cave (Fig. 1). Among the troglophiles, we identified four nominal species; *Tegenaria pagana* (Fig. 2a) is the most abundant species at cave entrances, corroborating previous results (Cuff et al., 2021; Gavish-Regev et al., 2021), *T. dalmatica* (Fig. 2b) from water cisterns ('En Lifta, Fig. 1 #23;'En Sarig, Fig. 1 #25), *T.* cf. *epacris* (Fig. 2c) from cave entrances, mainly at the Karmel mountain ridge caves (Sefunim, Fig. 1 #15; Ezba', Fig. 1 #17; and Horbat Ruma, Fig. 1 #12), and *T. angustipalpis* (Fig. 2d) inhabiting cave entrance at the upper Galilee of Israel (Shetula, Fig. 1 #1; Irav, Fig. 1 #2; Sharakh, Fig. 1 #4; Marva, Fig. 1 #6; Beit-Jann, Fig. 1 #7; Tefen, Fig. 1 #8; Hutat-Seter, Fig. 1 #9; and Kamon, Fig. 1 #10). We found two additional non-troglomorphic lineages that were not identified to species level and might represent undescribed species. All these species comprise a clade with all troglophile eye-bearing funnel-web spiders from our study (Fig. 3).

Among the troglobitic spiders found at the twilight and dark zones, we identified two distinct eyeless species (Figs. 3-4), one from A'rak Na'asane cave (Fig. 1 #18) located at the Judean desert and the other from Ornit cave (Fig. 1 #14) located at the Karmel mountain ridge. In the other 12 caves inhabited by eye-reduced troglobitic *Tegenaria* species, we found subtle changes that were not associated with many diagnosable variations of the male secondary genital organ, the pedipalp. However, we did find subtle but consistent morphological differences of eye phenotype, female epigynum (Fig. 4), and male RTA (see Taxonomy section for further details). We therefore used molecular methods to further test the relationships and species limits between those morphotypes.

3.2. Molecular sequencing and analysis of ddRAD

We recovered 382,027 RAD loci across all sequenced samples, but coverage of taxa per locus was not homogeneous. None of the loci were represented in all of the samples and only 515 had data for at least half of the samples. The phylogenetic analyses of the SNP datasets, either trimmed for sites with at least 50 % taxon occupancy or untrimmed dataset, recovered two clear clusters separated by a long branch; one cluster grouped all local troglobitic *Tegenaria* while the other included only local specimens with normal eyes, irrespective of locality or geographic proximity between clades (Fig. 3 and Appendix 1, respectively). A heatmap with the distribution of shared loci across samples showed that samples in the local troglobitic clade *s. lat.* (All local troglobitic species) shared more RAD loci with other local troglobitic samples and almost none with the local normal eyes specimens (Fig. 3, inset).

To further investigate the evolutionary structure of local troglobitic specimens, we reran ipyrad to include only 19 samples from the local troglobitic clade *s. lat.* (namely: *T. gainesteros* sp. nov., *T. frumkini* sp. nov., *T. naasane* sp. nov., *T. ornit* sp. nov., *T. trogalil* sp. nov., *T. yaaranford* sp. nov., and *T. yotami* sp. nov.), thus avoiding potential non-homologous loci caused by the distantly related troglophilic *T. pagana* and *T. dalmatica* samples. These smaller datasets recovered 198,785 RAD loci and much better taxonomic coverage per locus, with 69,131 loci exhibiting at least 50 % taxon occupancy. Phylogenetic analyses under various missing data threshold showed similar relationships to the broader analysis (Fig. 4, Appendix 1), differing mostly on support values and the position of the completely blind species from Ornit (Fig. 1 #14) and A'rak Na'asane (Fig. 1 #18) caves.

Both trimmed and untrimmed SNP datasets (Fig. 3 and Appendix 1, respectively), representing 58 individuals of the eye-bearing and reduced-eyes *Tegenaria* local species, as well as the selected 19 specimens of the local troglobitic clade *s. lat.* only (Fig. 4 and Appendix 2), strongly support eight clades of the local troglobitic species. Of the eight clades, four clades represent the Judean Mountain caves (Figs. 1, 4, #19–20, and #25–27), a clade for each cave (with the exception of two

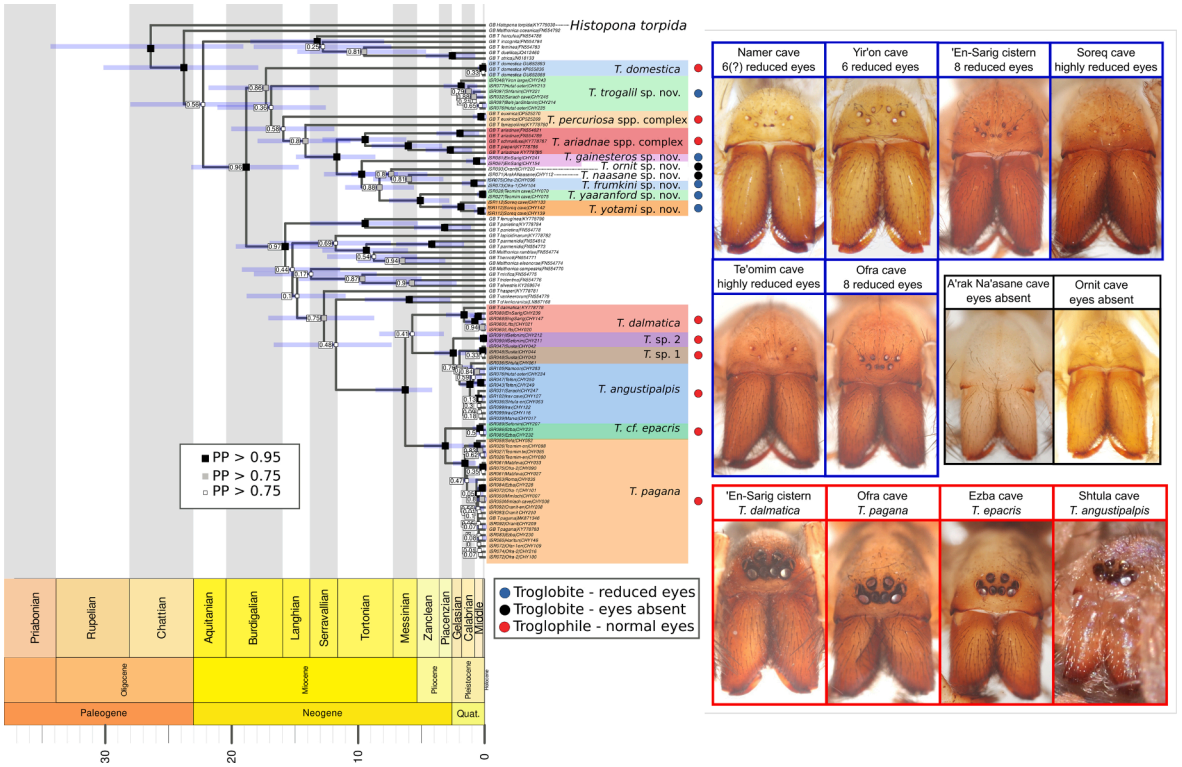

Fig. 5. Bayesian dated tree topology based on COI of reduced-eyes (blue dots) and eyeless (black dots) *Tegenaria* present at the deep sections of the caves and eye-bearing *Tegenaria* present at cave entrance (red dots). Nodes with posterior probability (PP) greater than 0.95 shown with black squares. Lower values indicated with gray and white squares with their associated values. Bars over the notes represent the 95 % highest probability density range of age of the nodes. (For interpretation of the references to colour in this figure legend, the reader is referred to the web version of this article.)

geographically closely related caves (Figs. 1, 4, #19–20) which are represented by one clade). Two additional clades represent the completely blind species from Ornit cave and A'rak Na'asane cave (Figs. 1, 4, #14, 18 respectively). The remaining two clades represent the eye-reduced spiders of the Galilee caves (three western caves, Figs. 1, 4, #2–4 and three eastern caves, #5, 7, 9). Depending on the resolution of the analyzed dataset, the two completely blind species are resolved at an intermediate position between the reduced-eye *Tegenaria* of the Galilee northern clade and the Judean southern clade (Appendix 2), or as the sister species to each of the clades. The latter topology is consistent with the geographic distributions of the different cave localities (Fig. 4).

3.3. Sequencing and analysis of COI locus

The phylogenetic tree of COI barcoding (Fig. 5) recovered a similar topology to the ddRAD sequencing (Figs. 3-4), with local troglobitic and troglophilic specimens forming distinct clades. The COI barcoding sequences of *T. pagana* and *T. dalmatica* from GenBank and our sequences of *T. pagana* and *T. dalmatica* fall together, respectively, in the same clades, supporting our morphological identification of the local troglophile specimens (Fig. 5). For the troglobitic species, *T. trogalil* sp. nov. was sister to a clade composed from the rest the local troglobitic species complex, the *T. ariadnae* species complex (represented in our phylogeny by *T. ariadnae* Brignoli, 1984, *T. schmalfussi* Brignoli, 1976 and *T. pieperi* Brignoli, 1979) and the *T. percuriosa* species complex (represented in our phylogeny by *T. faniapollinis* Brignoli, 1978 and *T. euxinica* Dimitrov 2022).

Estimation of divergence time recovered, based on the relaxed tree (Fig. 5, Supplementary Fig. S1), a median age of ca. 10 (9.7) mya for the local troglobitic clade *s. str.* (The "Judean + Karmel" troglobite clade formed by the species *T. gainesteros* sp. nov., *T. frumkini* sp. nov., *T. naasane* sp. nov., *T. ornit* sp. nov. *T. yaaranford* sp. nov., and *T. yotami* sp. nov.) (95 % highest posterior density interval: ca. 7–12.5 mya).

3.4. Integrative taxonomy of cave dwelling Tegenaria from Israel

Both ddRAD sequencing and COI barcoding analyses congruently recovered the local troglobitic and troglophilic *Tegenaria* to belong to two distantly related lineages. Yet, since COI unites the western and eastern Galilee into one clade, we treated the Galilee clade as one species, with the understanding that future sampling efforts may uncover additional species relationships within the geographically and morphologically defined Galilee clade. To formalize the outcomes of the molecular analyses and morphological findings, we describe below (See Taxonomy section) seven new species of troglobitic *Tegenaria* that exhibit diagnosable morphological differences from one another, as well as from congeners.

4. Discussion

Understanding current distributions in the light of historical biogeography, major climatic changes and geological events poses a scientific challenge. Here, we investigated the evolutionary and biogeographic history of the cave fauna of Israel through the lens of its troglophilic and troglobitic funnel-web spiders. Thereafter, we assessed congruence with competing models for speciation in the cave-adapted *Tegenaria*.

One established model of speciation in caves commences with divergent populations of the same species with polymorphic traits; some populations have troglomorphic phenotypes, such as eye-reduction, whereas others have normal eyes (Fig. 6a). The absence of speciation may be detected by the lack of reproduction isolation, and minimal (or no) genetic distance between eye-bearing and troglomorphic populations, as exemplified by the well-studied Mexican cavefish system (*Astyanax mexicanus* (De Filippi, 1853); Bradic et al., 2012; Strecker et al., 2003). Another model postulates that the caves are inhabited by

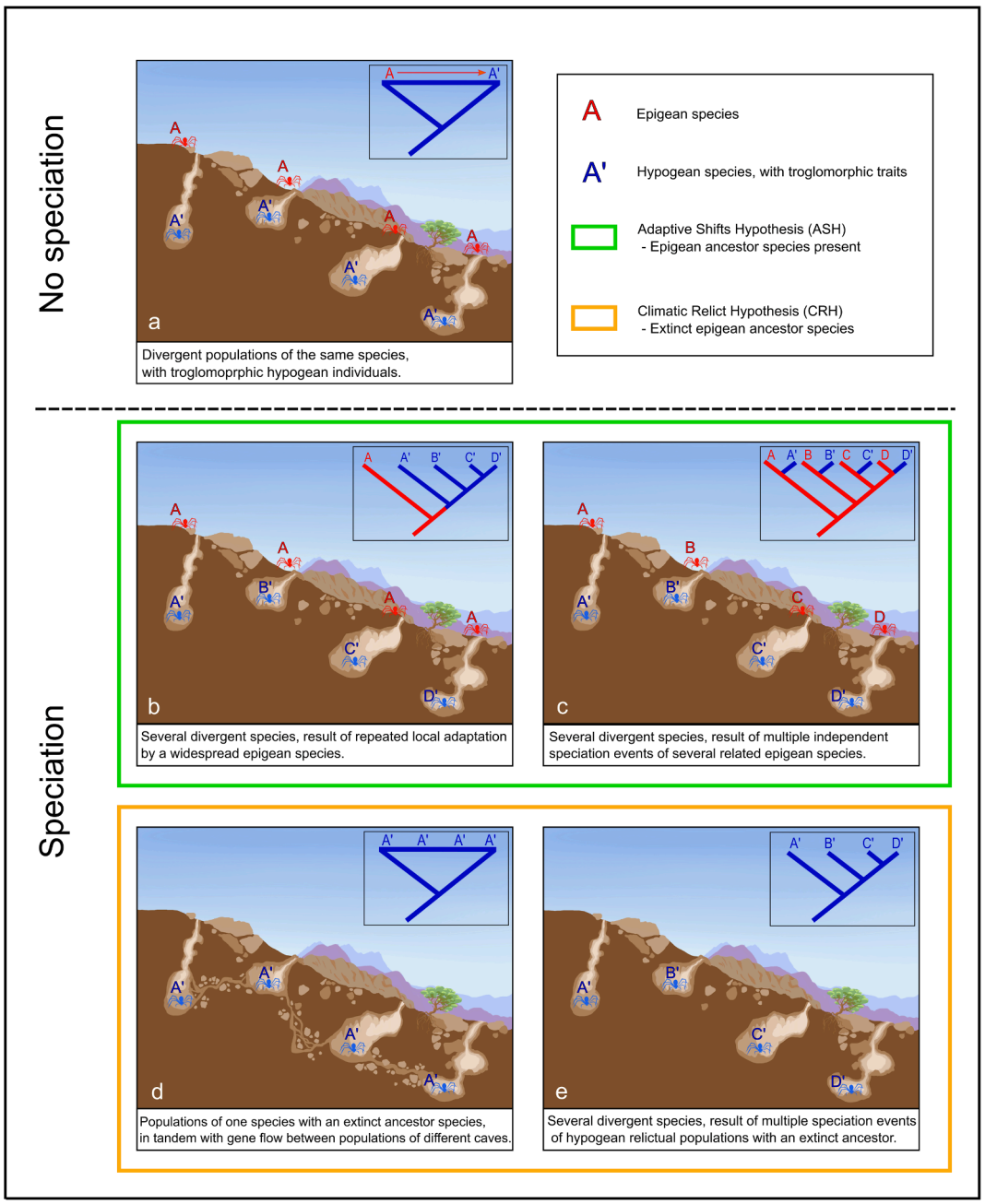

Fig. 6. Divergence scenarios (**a-e**) and speciation mechanisms of cave-dwelling species (modified from Trontelj, 2018).

several divergent species descending from a widespread epigean species that underwent local adaptation to the cave environment (Fig. 6b). A modification of this model postulates that the caves are inhabited by different species descending from several related epigean species, as a result of multiple independent speciation events (Fig. 6c), as exemplified by spiders of the genus *Dysdera* Latreille, 1804, from the Canary Islands (Arnedo et al., 2007). These models invoke speciation in parapatry and are in agreement with the ASH.

Alternative models for cave colonization postulate that different extant cave populations descend from an extinct surface ancestor species, with daughter populations maintaining gene flow between different caves (Fig. 6d). A modification of this scenario postulates that the extant cave species, descended from an extinct surface ancestor, are a result of multiple speciation events that separate subterranean relictual populations (Fig. 6e). For these scenarios, the sister species is inferred to be completely extinct or found in a remote habitat with climatic conditions that are different from that of the current epigean habitat. Such models are in agreement with the CRH.

Overall, the tree topology and estimation of divergence times we recovered were more consistent with the CRH, wherein well-differentiated troglobitic species probably descended from one or more epigean ancestors, which subsequently underwent local (and possibly global) extinction (Fig. 7). With the exception of two groups of geographically proximate cave sites, we found strong evidence for cessation of gene flow between several anatomically distinct morpho-species of *Tegenaria*. Seven of these microendemic species are newly described here. All troglobite *Tegenaria* found in Israel are part of a clade distantly related to the troglophile species found at each cave entrance. A local closest sister taxon to the troglobitic clade *s. lat.* remains unknown; Yet, a combination of morphological approaches and COI barcoding, suggests relationship to an eastern-Mediterranean species, the *T. ariadnae* and *T. percuriosa* species complexes, rather than to the

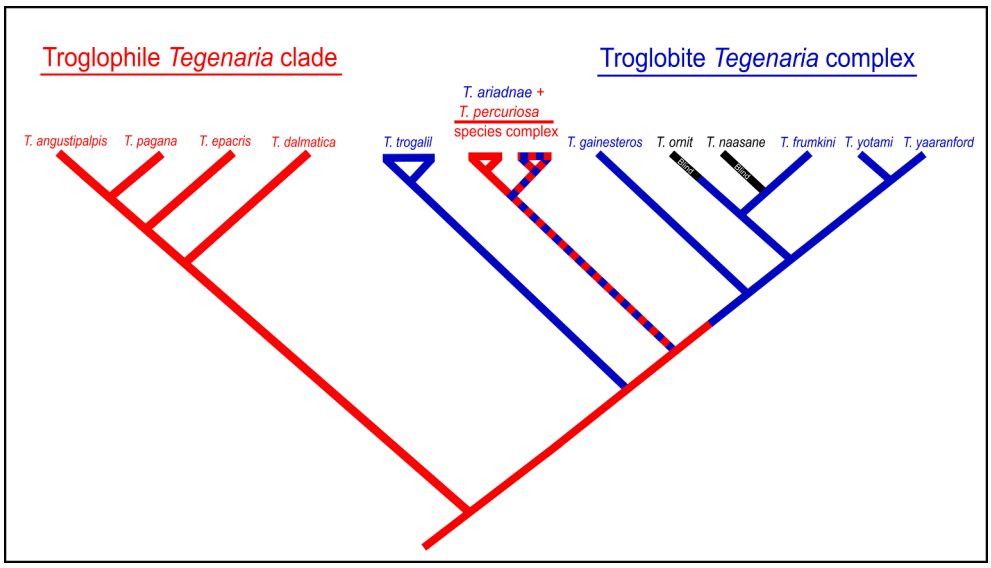

Fig. 7. Schematic cladogram summarizing divergence of troglophilic and troglobitic *Tegenaria* clades: reduced eyes (blue), eyeless (black) and eye-bearing *Tegenaria* (red). Dashed line represents a hypothesized sister clade, absent from the region. (For interpretation of the references to colour in this figure legend, the reader is referred to the web version of this article.)

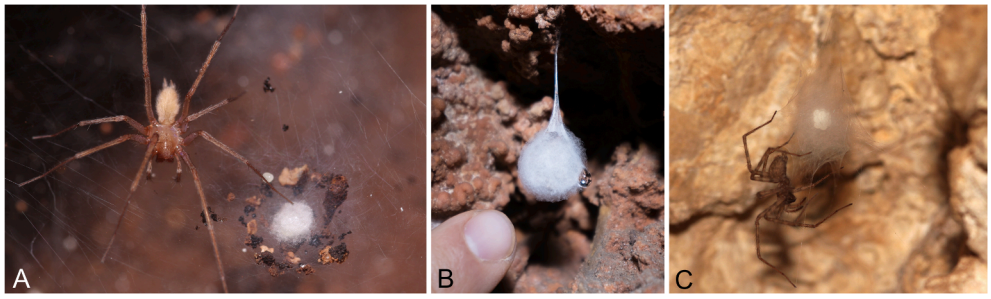

Fig. 8. *Tegenaria* egg sac. A. Adult female of the blind *Tegenaria ornit* sp. nov. from Ornit cave. Note the egg sac on the web, surrounded by soil particles. B. Egg sacs of *Tegenaria* sp. from cave twilight zone, suspended in the air on silken string. The egg sac is infected by mold (photograph: B. Langford). C. Female of *T. pagana* from Ezba' cave, depositing eggs and wrapping in silk, before hanging the egg sac from the cave wall nearby the female sheet web.

sympatric troglophilic species. At present, we cannot rule out the possibility of undiscovered, closely related sympatric troglophilic or epigean Tegenaria in Israel, though sampling density of our surveys in the past five years renders the incidence of undiscovered troglophilic sister species unlikely.

Agelenid egg sacs are usually suspended in the air on silken string (Toft and Lubin, 2018) as seen in *T. angustipalpis* and *T. pagana* in cave entrances (Fig. 1c). We observed egg sacs of four of the seven new species (i.e., *T. frumkini* sp. nov., *T. ornit* sp. nov., *T. trogalil* sp. nov. and *T. yaaranford* sp. nov.). In all four troglobitic species, the egg sacs were deposited directly on their sheet-webs (Fig. 1e, Fig. 8a). Suspension of the egg sacs in the air hypothesized to be an anti-predator behavior rather than coping with climatic conditions (Toft and Lubin, 2018). This hypothesis may be relevant for outside caves and cave entrance habitats where eggs' predators, like mites and ants, are more abundant. However, under cave conditions, where high humidity or even constant water flow from the cave walls may cause mold infection on hanging egg sacs (Fig. 8b, compare to Fig. 1c, and Fig. 8c), depositing egg sacs on the sheet-web may allow troglobitic *Tegenaria* species to nurse their egg sacs more easily and prevent mold infection. A survey of egg sac oviposition behavior of other troglobitic spiders, and in particular in the suggested sister species belonging to the *T. ariadnae* species complex, may shed light on this phenomenon.

The *Tegenaria ariadnae* species complex currently consists of five species known from caves and cave entrances, located in the vicinity of the Mediterranean Sea (three from Crete: *T. ariadnae*, *T. schmalfussi* and *T. pieperi*; one from Libya: *T. vallei* Brignoli, 1972; and one from southern Turkey; *T. lazarovi* Dimitrov, 2020) (Dimitrov, 2020). Some of these species are known to bear moderately reduced eyes, but their eyes are noticeably more developed than those of the Israeli troglobitic *Tegenaria*. *Tegenaria faniapollinis*, of the *T. percuriosa* species complex, is troglophilic and does not exhibit eye reduction (Lecigne, 2021). In addition to morphological similarities between the Israeli troglobitic species and some of the species in the *Tegenaria ariadnae* species complex (see Taxonomy, below), analyses of COI support their phylogenetic proximity, but these taxa were not available for sampling in our ddRAD sequencing analyses. Notably, the most extreme troglomorphism we observed (i.e., complete absence of eyes) was associated with the Ornit (Fig. 1 #14) and A'rak Na'asane (Fig. 1 #18) caves as part of the "Judean + Karmel" troglobitic clade *s. str.*, which are genetically distinct, based on COI phylogeny, from the *T. trogalil* complex and the *T. ariadnae* and *T. percuriosa* species complex.

Within spiders, empirical cases that are consistent with the ASH are known for a few troglobites, such as the Canary Island *Dysdera* woodlouse spiders (Arnedo et al., 2007). Spiders of the genus *Dysdera* Latreille, 1804, known from the Canary Islands (Arnedo et al., 2007), are a good example of an adaptive radiation of troglobite species inhabiting caves parapatrically with respect to one or more epigean ancestor. Similar phenomena are also found in the cave isopod *Asellus aquaticus* (Linnaeus, 1758) (Turk et al., 1996) and in the harvestman genus

Sclerobunus Packard, 1877 (Derkarabetian et al., 2010). By contrast, the monotypic spider *Trogloraptor marchingtoni* Griswold, Audisio & Ledford, 2012 (Griswold et al., 2012) represent an extreme scenario of an isolated and relictual troglobite species, with no sister species in the epigean vicinity. Yet, it is not always possible to find evidence for either ASH or CRH, especially when the divergence between sister species is recent, and the within population variance is small, such as in the parthenogenetic lineage of the Levantine whip spiders, of the genus *Sarax* Simon, 1892 (Baker et al., 2022) which inhabits mainly manmade ancient water cisterns, spring tunnels and rock-cut caves in the Mediterranean part of Israel.

Understanding the broader biogeographic and phylogenetic history of the group will require denser sampling of *Tegeneria* throughout the Mediterranean. The complex paleogeographic history of the Mediterranean region accompanied with climate changes drove dispersal events and biotic exchange between disjunct realms. Evidence of large scale dispersal between north Africa and Eurasia during the late Miocene ~ 9–5.3 mya through the Levantine corridor (Tchernov, 1988) may explain the current distribution of *T. ariadnae* species complex, spreading from Libya, Israel, Crete, and Turkey. Nonetheless, the drastic lowering of the sea level during the Messinian salinity crises occurred at the terminal stage of the Miocene ~ 5.3 mya, creating an inter-Mediterranean land bridge (Tchernov, 1988) enabling dispersal and colonization of isolated Mediterranean islands such as Crete and Cyprus (Dubey et al., 2007). The divergence of the Galilee clade from clade with the other local troglobitic species, *T. ariadnae* and *T. percuriosa* species complexes, was estimated by us as mid- to early Miocene (12–20 mya) and may have been precipitated by a marine transgression through Yizre'el valley ~ 9–7 mya, when the Mediterranean Sea was connected to the Dead Sea (Frumkin et al., 2020; Langford et al., 2019), explaining also the remote distribution of *T. naasane* at the northern Judean desert, which was located at the shore of the flooded Dead Sea Rift. The rising of the sea to the present level at the beginning of Pliocene ~ 5 mya may explain the present vicariance distribution pattern of the species complex members.

Across the sites surveyed herein, we discovered only two cases where a species was discovered in multiple cave sites. *Tegenaria frumkini* sp. nov. was discovered in two cave sites in the Ofra cave system. This species inhabits caves in the Ofra karst basin, that comprise more than 40 caves within 5 km^2. At least some of the caves in this region are connected via fractures within the epikarst (Langford et al., 2019) that may allow gene flow between cave populations. Ongoing efforts aim to investigate whether the *Tegenaria* of this cave system represents gene flow or incipient speciation across isolated sites. A more complicated example is that of *Tegenaria trogalil* sp. nov., that is found in several caves throughout the Galilee. This species presents an ambiguous topology. Although the ddRAD sequencing dataset and morphological analyses support two distinct clades within the Galilee caves, the COI gene tree did not recover this topology. Instead, COI barcoding united the Galilee specimens on one long branch. This conflict may be due to limitations of a single-locus approach, differences in representation of *Tegenaria* species and localities between datasets, or the information content of the ddRAD SNP dataset. Future efforts to infer gene flow and test species delimitation within the Galilee and Ofra cave systems must emphasize denser population sampling, in tandem with genomic approaches, for *T. trogalil* sp. nov. and *T. frumkini* sp. nov., respectively.

The discovery of the seven *Tegenaria* microendemics adds to several examples of relictual species among the fauna of Israel. Disparate origins of these relicts likely reflect the complex paleogeographic history of the Mediterranean region. The more common source of the relicts are lineages of Palearctic origin, which represent a species expansion to the region during periods of humid climate. Additional climatic changes such as desiccation can cause local extinction events, leaving behind relictual populations in suitable habitats such as fluvial refugia, high mountains in the Mediterranean region and rock crevices habitats in the Negev desert. These populations often represent high endemism and speciation processes; examples are the rediscovered frog *Latonia nigriventer* Mendelssohn and Steinitz, 1943 (Biton et al., 2016) and dozens of plant species (Danin, 1999). Less common are lineages which expanded to Israel from the south, during hot and humid periods, which found refugia in suitable habitats during climatic changes. The African tree, *Faidherbia albida* (Delile) A. Chev. exemplifies a tropical element that expanded to the region during the Miocene, and exhibiting today a relictual distribution in Israel as a result of climate change during the Pliocene (Zohary, 1962). A'rak Na'asane cave, a unique hot and humid cave, surrounded by desert (Aharon et al., 2019; Frumkin et al., 2018) serves as a unique refugium, harboring a relictual harvestman (*Haasus naasane* Aharon et al., 2019). This species belongs to an isolated genus of a family that is found mostly in Sub-Saharan Africa (Aharon et al., 2019). The same desertic cave is home to the possible mesic relicts, such as the blind troglobitic *Tegenaria naasane* sp. nov..

5. Conclusion

The phylogenetic and biogeographic history of troglobitic Israeli *Tenegaria* accords with a scenario of *in situ* speciation of cave microendemics, followed by local extirpation of epigean counterparts. These lines of evidence substantiate the Climatic Relict Hypothesis for this component of the Levantine arachnofauna. Future biodiversity discovery efforts are anticipated to identify other microendemic components of the Levantine arachnofauna that may be of high priority for conservation efforts.

6. Taxonomy

Family **Agelenidae** C.l. Koch, 1837.

Genus ***Tegenaria*** Latreille, 1804.

Tegenaria Latreille, 1804: 134.

Type species: *Araneus domesticus* Clerck, 1757, by subsequent designation of Kluge (2007).

A detailed diagnosis for the genus is given by Bolzern et al. (2013), including the main following characters which fits well with all the seven new species described herein: 1. all leg trochanter straight or slightly curved; 2. leg patellae with two dorsal but no lateral spines; 3. absence of ventral spines at all leg tarsi; 4. male pedipalp with lateroventral ridge on RTA, filiform embolus, lamelliform conductor with a mostly simple ventral terminal ending, and elongated MA with distal sclerite; 5. female epigynum with a separated median region and vulva without either diverticula or long appendages at any duct. The colulus, which is usually developed as trapezoidal plate in the genus *Tegenaria*, is inconspicuous in the Israeli troglobite species. The males described here, share some similarities with cave-dwelling species in *T. ariadnae* species complex, especially with *T. schmalfussi* such as the shape of the conductor, a hook or a sickle shape, with a simple terminal end (not bifid). The females described here, also share some similarities with species in *T. ariadnae* species complex, especially with *T. lazarovi* and *T. ariadnae*, such as the shape of the epigynal median plate, the lateral margins and the simple globular receptacles. Some other species may also belong to *T. ariadnae* species complex, as *T. elysii* and *T.averni*, but since no male were described for those species by Brignoli, more data is needed. These shared morphological characters are also reflected in the genetic distance, as can be seen in the above phylogenetic section (Fig. 5), showing *T. ariadnae* complex (represented in our COI analysis by three species, namely: *T. ariadnae*, *T. schmalfussi* and *T. pieperi*) and *T. percuriosa* complex (Dimitrov et al., 2022) (represented in our COI analysis by two species, namely: *T. euxinica* and *T. faniapollinis*) as sister to the Israeli troglobitic complex, excluding *T. trogalil*. Yet, since the species of *T. percuriosa* complex share only few characters with the Israeli troglobitic species (e.g., long cymbium), they are not compared in detail in the diagnosis.

Morphologically, males of *T. angustipalpis* probably belongs to *T. percuriosa* species complex (Dimitrov et al., 2022), however, in our

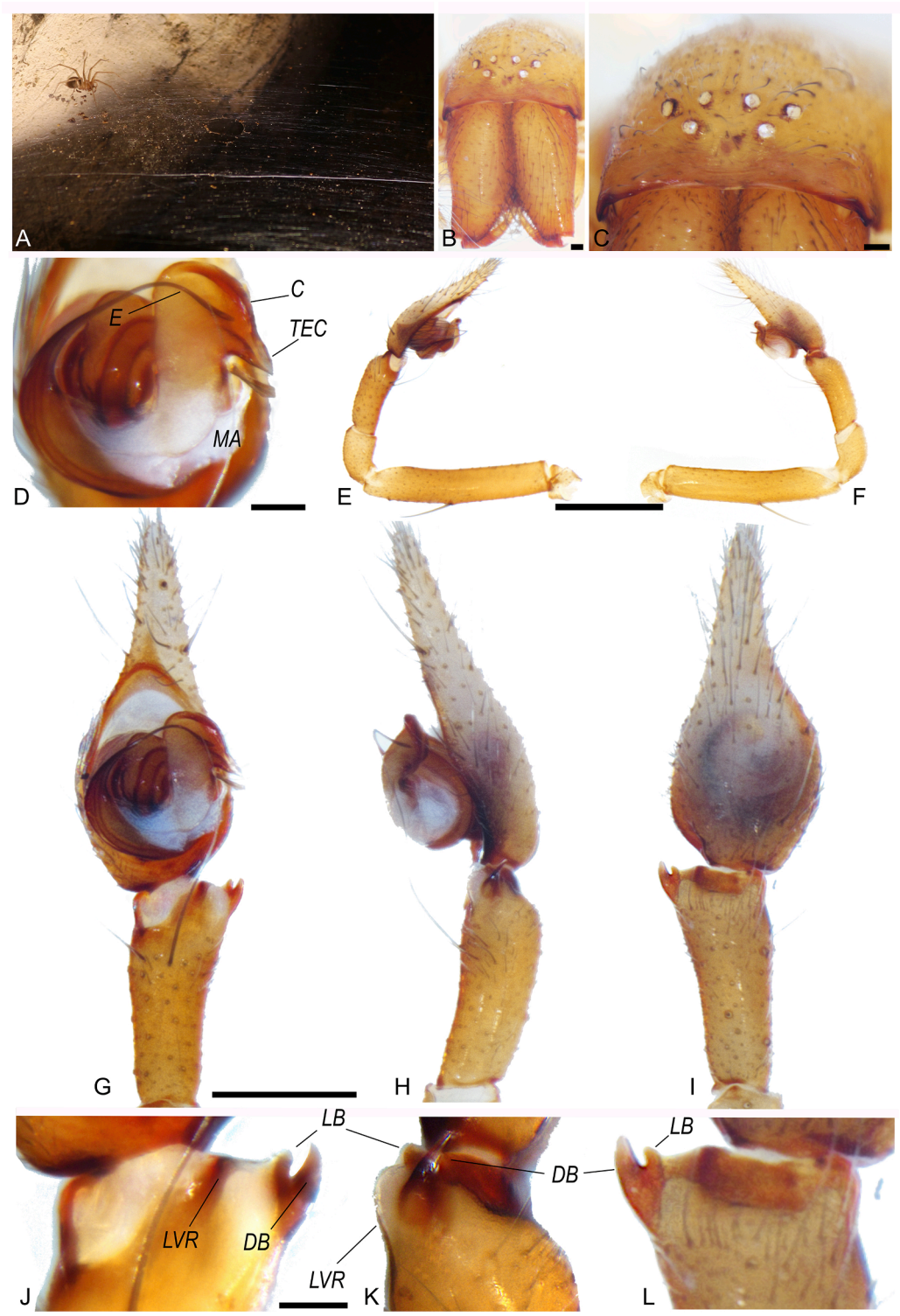

Fig. 9. *Tegenaria trogalil* sp. nov. **A.** Live habitus, Yir'on cave. **B-L.** Male holotype (HUJ - INVAr 20378). **B.** Carapace and chelicera, frontal view. **C.** Eyes region, frontal view (notice AME absent). **D-I.** Male left pedipalp, ventral view (**D, G**), prolateral view (**E**), retrolateral view (**F, H**), dorsal view (**I**). **J-L.** Male left pedipalp, RTA in ventral (**J**), retrolateral (**K**) and dorsal views (**L**). *C*, conductor; *DB*, dorsal branch; *E*, embolus; *LB*, lateral branch; *LTR*, lateroventral ridge; *MA*, median apophysis; *TEC*, terminal end of conductor. Scale bars: B-D, J-L 0.1 mm; E-F 1 mm; G-I 0.5 mm.

COI tree (Fig. 5) all the sequenced specimens of *T. angustipalpis* were females and juveniles and they belong to a distantly related clade, with the other troglophilic Israeli *Tegenaria*. Dimitrov et al. suggested that the described male and female of *T. angustipalpis* does not belong to the same species, since they were not collected from the same locality and were tentatively considered as a pair by Levy (Dimitrov et al., 2022; Levy, 1996). Unfortunately, we could not test this as we did not have males that could be used for molecular analysis.

Tegenaria trogalil sp. nov. Aharon & Gavish-Regev.

LSID:urn:lsid:zoobank.org:act:A84AE14E-47AB-43BA-A628-8C048361C514.

(Figs. 4, 9–11).

Type material

Holotype. ISRAEL. upper Galilee: Yir'on cave, 528 m a.s.l., dark zone, (33.0679°N, 35.4665°E), G. Gainett, S. Aharon, J.A. Ballesteros, P. P. Sharma leg., 26/VII/2018, in 96 % ethanol, ♂ (HUJ - INVAr 20378).

Paratypes. ISRAEL. upper Galilee: Same data as holotype, in 96 % ethanol, 3♀♀ (HUJ - INVAr 20380–20382). Same locality as holotype, S.

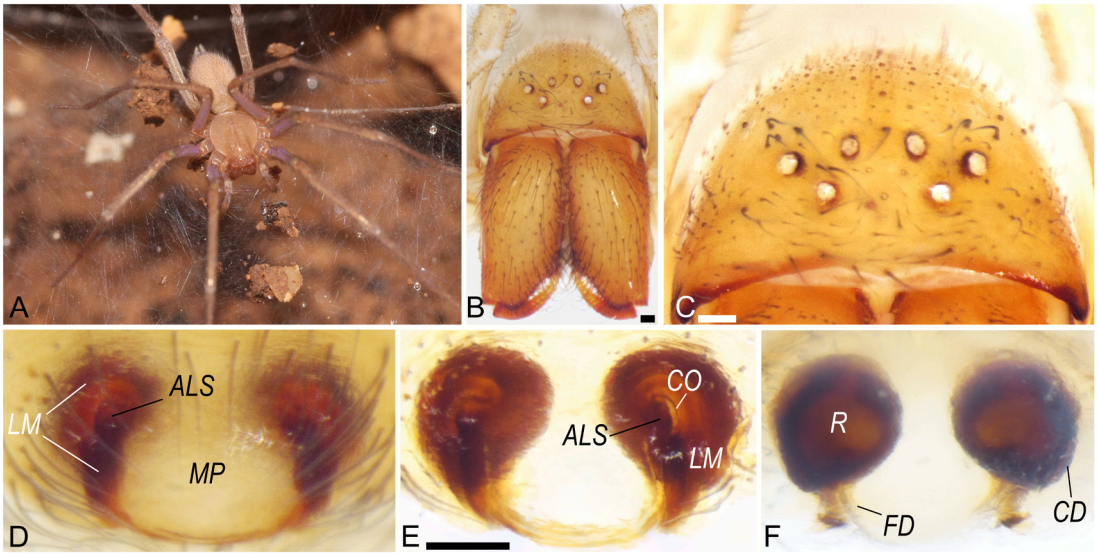

Fig. 10. *Tegenaria trogalil* sp. nov. **A.** Live habitus (female), Yir'on cave. **B-F.** Female paratype (HUJ - INVAr 20381). **B.** Carapace and chelicera, frontal view. **C.** Eyes region, frontal view (notice AME absent). **D-E.** Epigynum, ventral view, before (**D**) and after (**E**) clearing. **F.** Vulva, dorsal view. *ALS*, anterolateral sclerite of median plate; *CD*, copulatory duct; *CO*, copulatory opening; *FD*, fertilization duct; *LM*, lateral margin of epigynum; *R*, receptaculum. Scale bars: B-F 0.1 mm.

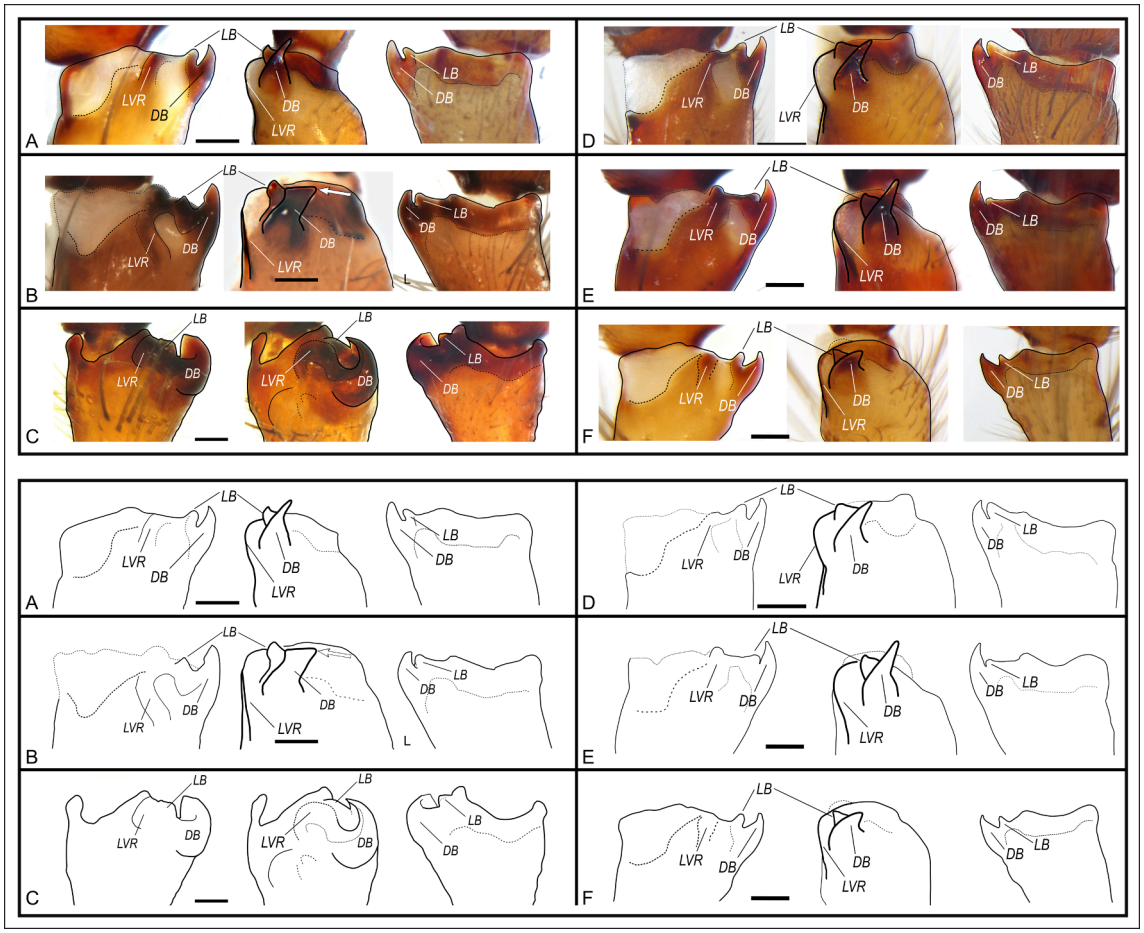

Fig. 11. Projected line drawings on pictures, and line drawings alone (below) of males left RTA. Pedipalp are from left to right: ventral, retrolateral and dorsal. **A.** *T. trogalil* sp. nov.; **B.** *T. ornit* sp. nov.; **C.** *T. naasane* sp. nov.; **D.** *T. frumkini* sp. nov.; **E.** *T. gainesteros* sp. nov.; and **F.** *T. yaaranford* sp. nov.

Aharon & E. Gavish-Regev leg., 28/V/2014, 1♂ (HUJ - INVAr 20424).

Other material examined:

ISRAEL. upper Galilee: Same locality as holotype, S. Aharon & E. Gavish-Regev leg., 28/V/2014, 1♀, 6 juveniles (HUJ - INVAr 20423), 1♀ (HUJ - INVAr 20425). Same locality, S. Aharon leg., 12/III/2014, 1♀, 3 juveniles, 1 sub-adult male (HUJ - INVAr 20426), 2♀♀ (HUJ - INVAr

20427), (HUJ - INVAr 20428). Same locality, S. Aharon leg., 18/VIII/2021, 1♂ (HUJ - INVAr 20444). Same data as holotype, in 96 % ethanol, 12 juveniles, 1 sub-adult male (HUJ - INVAr 20379). Hutat-Seter cave, 370 m a.s.l., (32.9417°N, 35.4758°E), S. Aharon & S. Ya'aran leg., 9/VIII/2018, in 96 % ethanol, twilight zone, 1♂ (HUJ - INVAr 20402), 1♀ (HUJ - INVAr 20403). Same data, dark zone, 1♂ (HUJ - INVAr 20432), 7♀ (HUJ - INVAr 20433–20439). Beit-Jann, Shfanim cave, 927 m a.s.l, dark zone, (32.9615°N, E35.3951°E), S. Aharon, S. Ya'aran, J.A. Ballesteros leg., 21/VIII/2018, in 96 % ethanol, 1♂ (HUJ - INVAr 20400), 4 juveniles, 1 sub-adult male (HUJ - INVAr 20401). Sharakh cave, 299 m a.s.l., (33.0740°N, 35.2378°E), S. Aharon & J.A. Ballesteros leg., 24/VII/2018, in 96 % ethanol, dark zone, 6♀♀ (HUJ - INVAr 20409–20414), 1 juvenile (20404), 1 sub-adult male (HUJ - INVAr 20415). Same locality, S. Aharon leg., 17/II/2020, 1♂ (HUJ - INVAr 20429), 1♀ (HUJ - INVAr 20430). Same locality and coll., 16/VIII/2021, 2♂ (HUJ - INVAr 20448–20449), 2♀ (HUJ - INVAr 20450–20451). Irav cave, 449 m a.s.l., (33.0799°N, 35.2285°E), S. Aharon leg., 22/VIII/2018, in 96 % ethanol, dark zone, 1♀ (HUJ - INVAr 20386), twilight zone, 1 juvenile (20404). Namer cave, 233 m a.s.l., (33.0782°N, 35.1906°E), S. Aharon, G. Gainett, J.A. Ballesteros, P.P. Sharma leg., 24/VII/2018, in 96 % ethanol, dark zone, 3♀ (HUJ - INVAr 20405–20407), 9 juveniles (20408).

Etymology

The species name is a combination of "troglobite", an obligate cave dwelling organism, and "Galilee", the geographic region in northern Israel, where the caves inhabited by the species are located.

Diagnosis

Males of *Tegenaria trogalil* sp. nov. are most similar to the species in the Israeli troglobitic *Tegenaria* species complex *s. s.* (*T. gainesteros* sp. nov., *T. frumkini* sp. nov., *T. naasane* sp. nov., *T. ornit* sp. nov. *T. yaaranford* sp. nov.) and to *T. schmalfussi*. No males of *T. yotami* sp. nov. have been found yet. The males can be hardly distinguished from *T. gainesteros* sp. nov., *T. frumkini* sp. nov., and *T. yaaranford* sp. nov., but differs from the other congeners by the combination of 1) RTA with a pointed, tusk-like dorsal branch, rather than a blunt edged dorsal branch in *Tegenaria ornit* sp. nov., a robust and heavily sclerotized RTA in *Tegenaria naasane* sp. nov., forming a "tilde"-like shape, and short blunt RTA in *T. schmalfussi* (Fig. 11), 2) conductor forms a hook-like shape, ends to a short, beak-like shape, rather than a sickle-shaped, terminally pointed in *T. naasane* sp. nov. and *T. schmalfussi*.

Females are similar to the species in the Israeli troglobitic *Tegenaria* species complex *s. s.* (except *T. naasane* sp. nov.) and to *T. lazarovi* and *T. ariadnae*. Females can be distinguished from *T. lazarovi* and *T. ariadnae* by 1) broader shape of epigynal median plate rather than anteriorly broad in *T. ariadnae*. 2) copulatory openings forming a crescent-like slit shape, while they are straight and perpendicular to the epigynal median plate in *T. lazarovi* and horizontaly opened in *T. ariadnae*. Females differ from the other Israeli troglobitic species by the combination of 1) pale region of median plate before clearing, forming a barrel-like shape, wider than long. 2) less prominent anterolateral sclerites, forming a rectangular median plate after clearing.

Description

Male (holotype (HUJ - INVAr 20378)):

Coloration. *Carapace* pale brown, anterior elevated region yellowish to light brown. *Abdomen* pale brown. *Colulus* inconspicuous. *Chelicerae* light brown. *Labium and Endites* light brown. *Sternum* pale with light yellow margins. *Legs* depigmented to pale yellow, femur of leg I-II light brown to reddish, femur of pedipalp light brown. *Chelicerae* length 1.17, retromargin teeth 5, promargin teeth 3. *Carapace* length 2.59, width 2.07. *Abdomen:* length 2.90, width 1.62. *Total length* 5.49. *Sternum* length 1.40, width 1.25. *Clypeus* length 0.20. *Eye diameters and interdistances* AME absent, ALE 0.06, PLE 0.06, PME 0.06, ALE-PLE 0.08, PME-PME 0.14, PME-PLE 0.12, PME-ALE 0.08. **Appendages**. *Pedipalp:* femur 1.64, patella 0.49, tibia 0.71, tarsus 1.26. *Leg I:* femur (fe) 4.83, patella (pa) 1.06, tibia (ti) 5.06, metatarsus (mt) 5.23, tarsus (ta) 2.36. *II:* fe 4.09, pa 1.00, ti 3.96, mt 4.25, ta 2.06. *III:* fe 3.66, pa 0.90, ti 3.27, mt 3.95, ta 1.73. *IV:* fe 4.39, pa 0.85, ti 4.33, mt 5.37, ta 2.15. **Pedipalp**. *RTA* with three sclerotized branches, Lateroventral ridge present. Ventral branch flat and less prominent, semisclerotized, continuing ventrally to a fine sclerotized lateroventral ridge. Dorsal branch prominent, tusk-like, protruding and pointed dorsodistally. Lateral branch smaller, protruding oppositely to dorsal branch. *embolus* moderately long and filiform. Originating at 9o'clock position, distal end at 2o'clock position. *conductor* hook-like, rounded distally. Distal and retrolateral margins folded all along to the terminal end of conductor. Terminal end pointed, somewhat robust, short beak-like shape, folded subtly at the distal and proximal margins, forming a slender groove along the folding. *MA* membranous, twisted distally, with distal sclerite somewhat flattened.

Male variation (paratype (HUJ - INVAr 20424)):

Coloration. *Carapace* pale brown, anterior elevated region yellowish to light brown. *Abdomen* pale brown. *Colulus* inconspicuous. *Chelicerae* light brown. *Labium and Endites* light brown. *Sternum* yellowish. *Legs* yellowish, femur of legs I-II and palps are light brown. *Chelicerae* length 1.14, retromargin teeth 4 or 5, promargin teeth 3. *Carapace* length 2.67, width 2.12. *Abdomen:* length 2.51, width 1.98. *Total length* 5.18. *Sternum* length 1.37, width 1.34. *Clypeus* length 0.19. *Eye diameters and interdistances* AME 0.05 (R) 0.02 (L), ALE 0.05, PLE 0.06, PME 0.06, AME-AME 0.09, AME-ALE 0.06, ALE-PLE 0.09, PME-PME 0.15, PME-AME 0.09 (R) 0.12 (L), PME-PLE 0.12, PME-ALE 0.10. **Appendages**. *Pedipalp:* femur 1.67, patella 0.50, tibia 0.68, tarsus 1.27. *Leg I:* femur (fe) 3.79, patella (pa) 1.10, tibia (ti) 4.85, metatarsus (mt) 5.14, tarsus (ta) 2.30. *II:* fe 3.69, pa 0.97, ti 3.80, mt 4.23, ta 1.93. *III:* fe 3.49, pa 0.84, ti 3.10, mt 3.91, ta 1.58. *IV:* fe 4.10, pa 0.82, ti 3.94, mt 5.27, ta 2.00.

Female (paratypes (HUJ - INVAr 20381), (HUJ - INVAr 20405)):

Coloration. *Carapace* pale yellow, anterior elevated region yellowish. *Abdomen* depigmented. *Colulus* inconspicuous. *Chelicerae* yellowish to light brown. *Labium and Endites* light brown. *Sternum* pale with light yellow margins. *Legs* depigmented to pale brown, femur of legs I-II yellowish to pale brown, femur of pedipalp light brown. *Chelicerae* length 1.22–1.62, retromargin teeth 5, promargin teeth 3. *Carapace* length 2.51–2.92, width 1.70–2.17. *Abdomen:* length 2.75–3.62, width 1.56–2.36. *Total length* 5.26–6.54. *Sternum* length 1.40–1.41, width 1.16–1.27. *Clypeus* length 0.19–0.23. *Eye diameters and interdistances* AME absent (diameter of the pigmented area is 0.04), ALE 0.04–0.05, PLE 0.06, PME 0.02–0.06, ALE-PLE 0.09–0.12, PME-PME 0.14–0.22, PME-PLE 0.13–0.21, PME-ALE 0.10–0.19. **Appendages**. *Pedipalp:* femur 1.31–1.72, patella 0.36–0.50, tibia 0.84–1.07, tarsus 1.10–1.58. *Leg I:* femur (fe) 3.57–4.64, patella (pa) 1.02–1.06, tibia (ti) 3.45–5.01, metatarsus (mt) 3.62–5.02, tarsus (ta) 1.98–2.69. *II:* fe 3.04–3.71, pa 0.80–0.97, ti 2.85–4.21, mt 2.96–4.66, ta 1.68–2.26. *III:* fe 2.85–3.66, pa 0.73–0.98, ti 2.47–3.64, mt 3.00–4.54, ta 1.43–1.90. *IV:* fe 3.41–4.06, pa 0.71–0.90, ti 3.37–4.85, mt 4.11–6.21, ta 1.67–2.10. *Epigynum* length 0.16–0.22, width 0.32–0.41. **Epigynum and vulva**. *Median plate* before clearing, with median pale region oval shaped, wider than higher or almost the same proportion. Anterolateral sclerite less prominent or protruding, forming a rectangular shape of the general median plate region after clearing. *Lateral margin* sclerotized, ear-like shaped, longer than wide. Semicircular anteriorly, forming a crescent-like slit copulatory opening, covered by the anterolateral sclerite of the median plate. Posteriorly somewhat covering in a thin sclerite layer the posteromargins of the median plate. *Vulva* receptacles globular and sclerotized, slightly pointed posteriolaterally, copulatory ducts not prominent, fertilization ducts represented by small, leaf-like appendages.

Remarks and general variation

Tegenaria trogalil sp. nov. comprise of specimens that were collected from western and eastern Galilee caves. Variation in morphological characters, especially eye reduction level and female epigynum, was observed between the caves, while high similarity is observed within specimens from the same cave. Females from the eastern Galilee caves (Yir'on cave, Hutat-Seter cave), show a wider median sclerite of

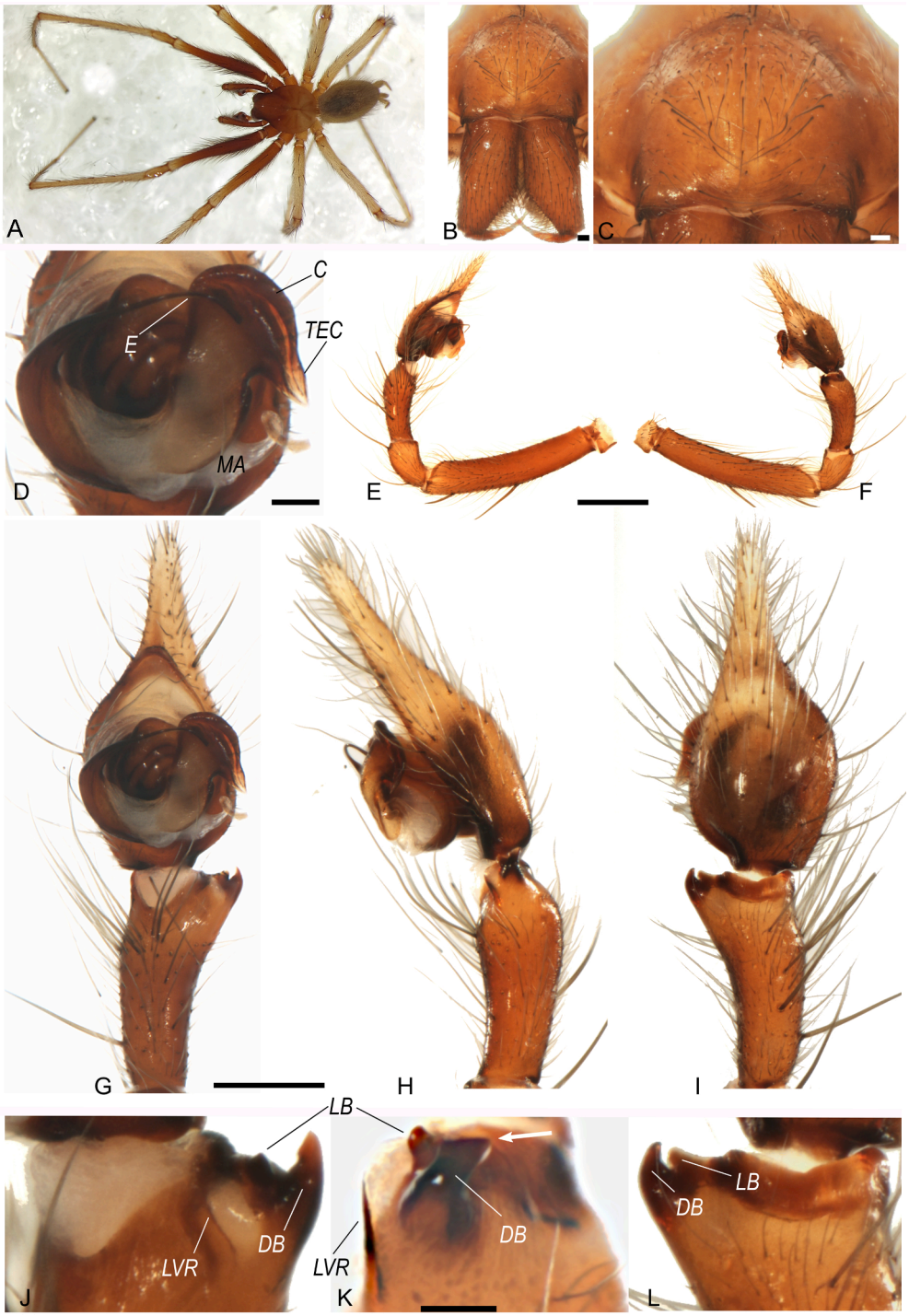

Fig. 12. *Tegenaria ornit* sp. nov., Male holotype (HUJ - INVAr 20453). **A.** habitus. **B.** Carapace and chelicera, frontal view. **C.** Eyes region, frontal view (notice all eyes are absent). **D-I.** Male left pedipalp, ventral view (**D, G**), prolateral view (**E**), retrolateral view (**F, H**), dorsal view (**I**). **J-L.** Male left pedipalp, RTA in ventral (**J**), retrolateral (**K**) and dorsal views (**L**). *C*, conductor; *DB*, dorsal branch; *E*, embolus; *LB*, lateral branch; *LTR*, lateroventral ridge; *MA*, median apophysis; *TEC*, terminal end of conductor. Scale bars: B-D, J-L 0.1 mm; E-F 1 mm; G-I 0.5 mm.

epigynum, and less prominent anterolateral sclerite and lateral margins of epigynum than females found at the western Galilee caves (Namer cave, Irav cave and Sharakh cave), (see Fig. 4). Eyes are reduced in all cave populations but vary between caves. From six eyes usually present in Yir'on cave population, lacking AME, and without any residual pigment at AME position (Figs. 5, 9B-C, 10B-C), to six reduced eyes and residual pigments at missing AME position in Namer cave population (Fig. 5), or eight reduced eyes present at Sharakh cave population.

Distribution and natural history

Known from caves located at the upper Galilee. *Tegenaria trogalil* sp. nov. is a troglobitic species, inhabiting caves situated in a range of elevation, from 233 m a.s.l. at Namer cave, situated 8 km of the Mediterranean Sea to 927 m a.s.l. at mount Meron. The species prefer relatively cold (17.3–22.7 °C) and humid (80–92.5 %) caves with active karst processes, which usually are inhabited by insectivorous bats, sometimes in large numbers and thick layer of guano as in Hutat-Seter, Irav and Sharakh caves, but can be found also in caves without bats like Beit-Jann cave. Other caves surveyed at the upper Galilee, which were less humid, were not found to be populated by *Tegenaria trogalil* sp. nov. The caves inhabited by this species can be represented by a multi-level structure, which may comprise moderately large halls as Irav, Sharakh, and Namer caves, by caves with a deep shaft and a large section as Hutat Seter cave, by a long (~150 m) tunnel shape as Yir'on cave, or by a simple round cavity as Beit-Jann cave. Two egg sacs were observed at

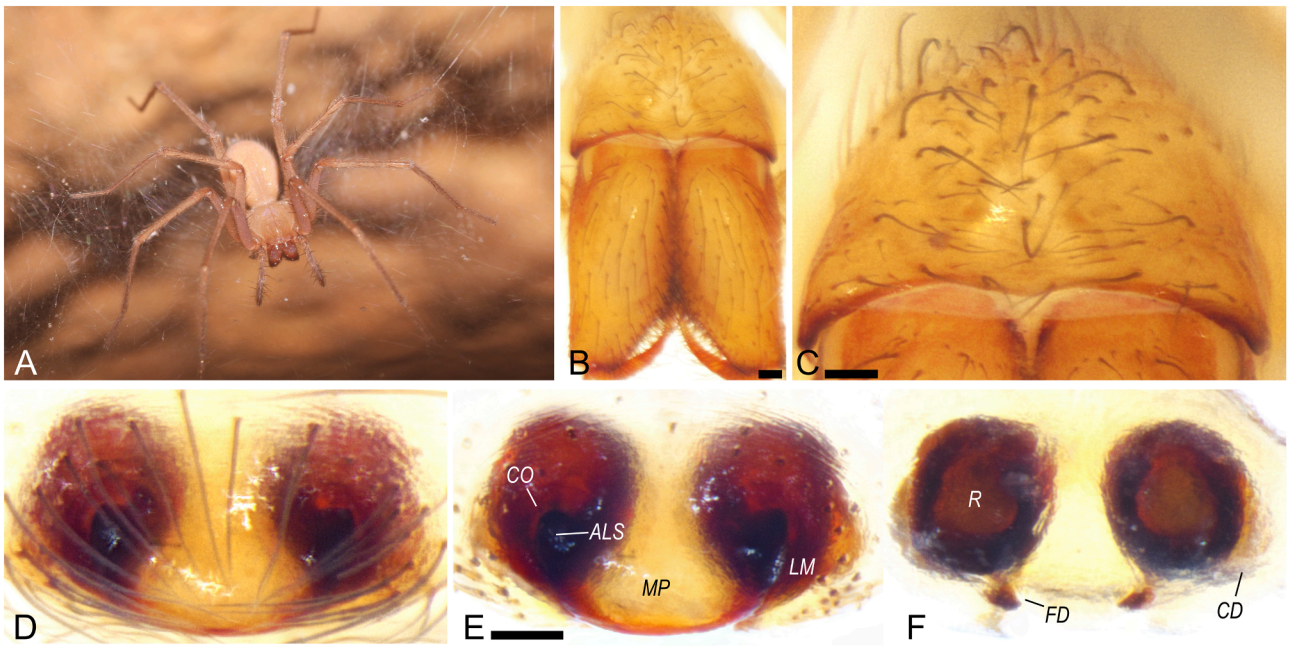

Fig. 13. *Tegenaria ornit* sp. nov. **A.** Adult female from Ornit cave, live habitus. **B-F.** Female paratype (HUJ - INVAr 20375). **B.** Carapace and chelicera, frontal view. **C.** Eyes region, frontal view (notice all eyes absent). **D-E.** Epigynum, ventral view, before (**D**) and after (**E**) clearing. **F.** Vulva, dorsal view. *ALS*, anterolateral sclerite of median plate; *CD*, copulatory duct; *CO*, copulatory opening; *FD*, fertilization duct; *LM*, lateral margin of epigynum; *R*, receptaculum. Scale bars: B-F 0.1 mm.

Yiro'n cave during the end of July 2018, one already hatched while the other was still closed. An unhatched egg sac found in Hutat-Seter cave on the 9th of August 2018 and three egg sacs in the same cave during a visit at the 16 of May 2022. All egg sacs were laid at the spider sheet-web (Fig. 1E), rather than ceiling hanged egg sacs of troglophile species found at the entrance of the cave. In addition, a juvenile was observed preying on a small isopod in Yir'on cave.

Tegenaria ornit sp. nov. Aharon & Gavish-Regev.

LSID:urn:lsid:zoobank.org:act:7A935650-BA55-4A42-87EE-E50731BB6F92.

(Figs. 1D, 8A, 11–13).

Type material

Holotype. **ISRAEL. Karmel mountain:** Ornit cave, 192 m a.s.l., dark zone, (32.7566°N, 34.9897°E), S. Aharon leg., 10/VIII/2022, ♂ (HUJ - INVAr 20453).

Paratypes. **ISRAEL. Karmel mountain:** Same locality as holotype, S. Aharon, G. Gainett, J. Ballesteros leg., 20/VIII/2018, in 96 % ethanol, 2♀ (HUJ - INVAr 20375–20376).

Other material examined:

ISRAEL. Karmel mountain: Same data as paratypes, in 96 % ethanol, 8 juveniles (HUJ - INVAr 20377). Same locality as holotype, S. Aharon & E. Gavish-Regev leg., 26/V/2021, 2 sub-adult males (HUJ - INVAr 20447).

Etymology

The species epithet, a noun in apposition, is derived from the name of the cave, which is the type locality of the species.

Diagnosis

The male of *Tegenaria ornit* sp. nov. is similar to the species in the Israeli troglobitic *Tegenaria* species complex *s. lat.* (*T. gainesteros* sp. nov., *T. frumkini* sp. nov., *T. naasane* sp. nov., *T. trogalil* sp. nov. *T. yaaranford* sp. nov.), and to *T. schmalfussi*. No males of *T. yotami* sp. nov. have been found yet. The male can be distinguished from other congeners by the combination of 1) RTA with blunt edge of dorsal branch rather than robust and heavily sclerotized RTA, forming a "tilde"-like shape as seen in *Tegenaria naasane* sp. nov., and a pointed, tusk-like dorsal branch in *T. gainesteros* sp. nov, *T. frumkini* sp. nov., *T. trogalil* sp. nov. and *T. yaaranford* sp. nov. (Fig. 11), 2) conductor forms a hook-like shape, ends to a short, beak-like shape, folded on distal and proximal margins, rather than a sickle-shaped, terminally pointed in *T. naasane* sp. nov. and *T. schmalfussi*.

Females of *Tegenaria ornit* sp. nov. are similar to the species in the Israeli troglobitic *Tegenaria* species complex *s. lat.* (except *T. naasane* sp. nov.) and to *T. lazarovi* and *T. ariadnae*. Females can be distinguished from *T. lazarovi* and *T. ariadnae* by 1) the shape of epigynal median plate, with more prominent and somewhat pointed anterolateral sclerites rather than straight in *T. lazarovi* and anteriorly broad median plate in *T. ariadnae*. 2) copulatory openings forming a crescent-like slit shape, while they are straight and perpendicular to the epigynal median plate in *T. lazarovi* and horizontaly opened in *T. ariadnae*. Females differ from the other Israeli troglobitic species by the combination of 1) anterolateral sclerites of median plate somewhat pointed to a short apex protruding anterolaterally (see Fig. 13 D-F), forming an anchor shape median plate. 2) pale region of median plate before clearing forming a juglet-like shape, rather than oval or trapezoidal shape as in the other Israeli troglobitic females. 3) distance between anterior edge of epigynum to anterolateral sclerites is wider than in the other females of the Israeli subterranean *Tegenaria* complex.

Description

Male (holotype (HUJ - INVAr 20453)):

Coloration. *Carapace* anterior elevated region brown, posterior region pale brown. *Abdomen* pale brown. *Colulus* inconspicuous. *Chelicerae* brown. *Labium and Endites* light brown. *Sternum* yellowish. *Legs* yellowish to light brown, femur of leg I-II light brown to reddish, pale distally. *Chelicerae* length 1.30, retromargin teeth 5 (R) or 6 (L), promargin teeth 3. *Carapace* length *3.20*, width *2.60*. *Abdomen:* length 3.00, width 1.90. *Total length 6.20*. *Sternum* length 1.50, width 1.20. *Eye diameters and interdistances* all eyes are absent. **Appendages**. *Pedipalp:* femur 1.85, patella 0.48, tibia 0.80, tarsus 1.30. *Leg I:* femur (fe) 4.90, patella (pa) 1.06, tibia (ti) 5.20, metatarsus (mt) 5.10, tarsus (ta) *2.95*. *II:* fe *5.04*, pa 1.00, ti 4.80, mt 4.85, ta 2.50. *III:* fe 4.01, pa 0.90, ti 3.80, mt 4.6, ta 1.90. *IV:* fe 4.25, pa 0.95, ti 4.80, mt 5.70, ta 2.30. **Pedipalp**. *RTA* with three sclerotized branches, Lateroventral ridge present. Ventral branch sclerotized, flat and less prominent, continuing ventrally to a fine sclerotized lateroventral ridge. Dorsal branch prominent, with blunt edge somewhat translucent distally, protruding dorsodistally. Lateral branch smaller, protruding oppositely to dorsal branch. *embolus*

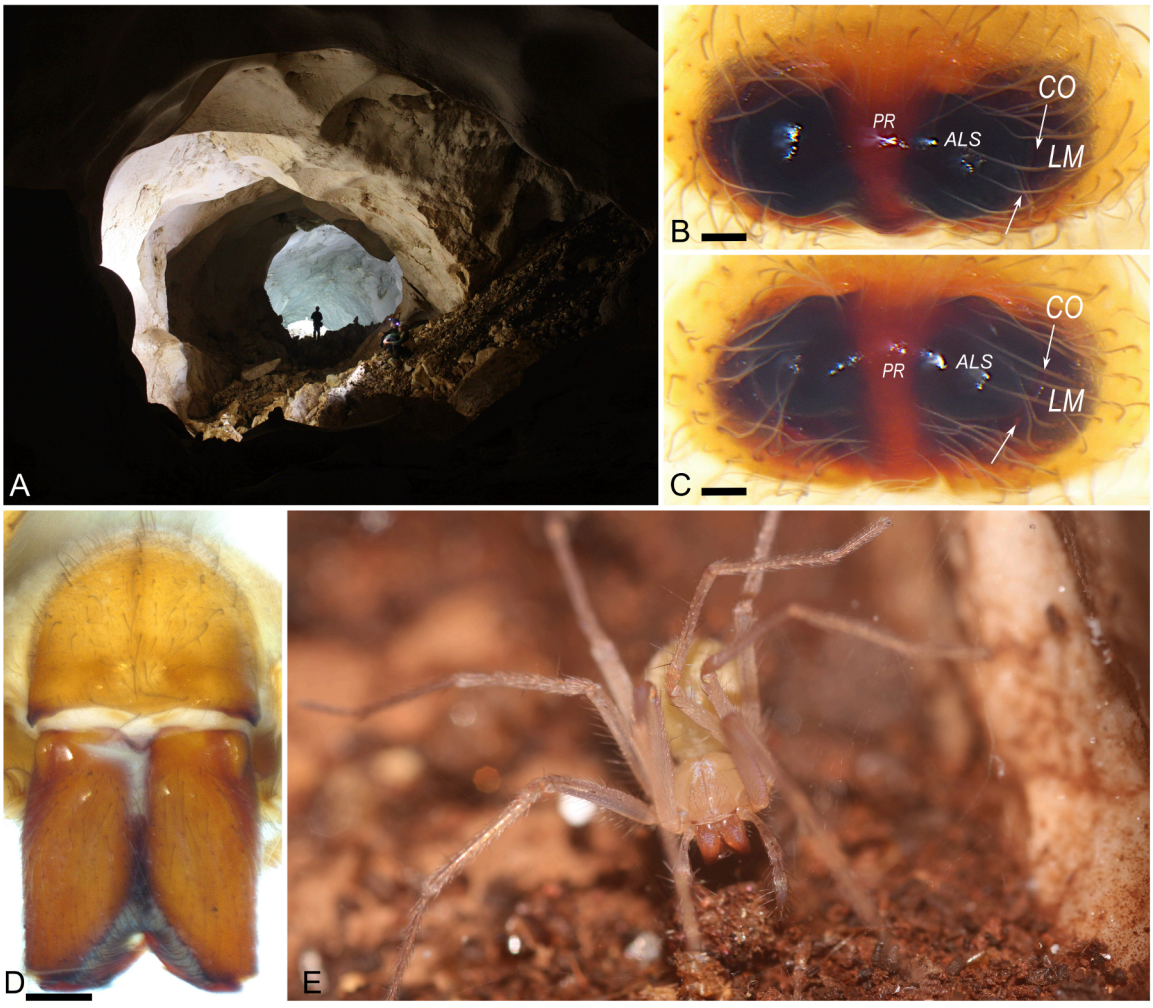

Fig. 14. *Tegenaria naasane* sp. nov. **A.** Large hall in A'rak Na'asane cave, Type locality of the species (Pic. B. Langford). **B-D.** Female holotype (HUJ - INVAr 20371). **B-C.** Epigynum, ventral view (**B**), lower angle posteroventrally (**C**). **D.** Carapace and chelicera, frontal view (notice all eyes absent). **E.** Live habitus. *ALS*, anterolateral sclerite of median plate; *PR,* pale region of median plate; *LM*, lateral margin of epigynum. Scale bars: B 0.5 mm; C-D 0.1 mm.

moderately long and filiform. Originating at 9o'clock position, distal end at 2o'clock position. *conductor* hook-like, rounded distally. Distal and retrolateral margins folded all along to the terminal end of conductor. Terminal end pointed, somewhat robust, short beak-like shape, folded subtly at the distal and proximal margins, forming a slender groove along the folding. This groove continues distally between the folded distal margin of conductor and a somewhat swollen ventral region of conductor. *MA* membranous, twisted distally, with distal sclerite somewhat flattened.

Female (paratypes (HUJ - INVAr 20375–20376)):

Coloration. *Carapace* pale yellow, anterior elevated region yellowish. *Abdomen* depigmented. *Colulus* inconspicuous. *Chelicerae* light brown. *Labium and Endites* light brown. *Sternum* pale with light-yellow margins. *Legs* pale yellow, femur of pedipalp pale to light brown. *Chelicerae* length 0.90–1.22, retromargin teeth 5, promargin teeth 3. *Carapace* length 2.41–2.74, width 1.44–2.08. *Abdomen:* length 2.7–4.08, width 1.82–2.91. *Total length* 5.11–6.82. *Sternum* length 1.26–1.52, width 0.96–1.34. *Eye diameters and interdistances* all eyes are absent. **Appendages**. *Pedipalp:* femur 1.09–1.1, patella 0.40–0.48, tibia 0.8–0.95, tarsus 1.1–1.42. *Leg I:* femur (fe) 3.40–4.14, patella (pa) 0.84–1.02, tibia (ti) 3.48–4.30, metatarsus (mt) 3.17–4.30, tarsus (ta) 2.22. *II:* fe 3.08–3.64, pa 0.78–1.00, ti 2.54–3.73, mt 2.89–3.92, ta 1.53–2.03. *III:* fe 2.74–3.49, pa 0.76–0.95, ti 2.54–3.16, mt 3.283.85, ta 1.60–1.70. *IV:* fe 3.38–4.22, pa 0.89–0.92, ti 3.44–4.31, mt 4.16–5.20, ta 1.63–2.00. *Epigynum* length 0.18–0.25, width 0.36–0.45. **Epigynum and vulva**. *Median plate* somewhat protruding. Pale region of median plate before clearing forming a juglet-like shape. Anterolateral sclerite of median plate somewhat pointed to a short apex protruding anterolaterally, forming an anchor or hammerhead shape median plate, hiding the copulatory openings. *Lateral margins* enfold the median plate dorsally. *Vulva* globular and sclerotized, surrounded dorsolaterally by semisclerotized copulatory ducts, visible at somewhat bottom view. Receptacles are reflected through epigynal plate, fertilization ducts represented by small appendages.

Distribution and natural history

Known only from the type locality. *Tegenaria ornit* sp. nov. is a troglobitic species, totally eyeless, missing all ocelli and eye pigmentation, found in the deep chamber of Ornit cave, located in the Karmel mountain ridge. The cave consists of two different ecological sections, one is a long corridor opened to the wadi with few large openings, inhabited by the troglophilic species *Tegenaria pagana*. The other is a deeper chamber, completely dark, accessible only through a narrow, long passage. The deep chamber (~60 m from the entrance) is seasonally inhabited by two insectivorous bat species, *Rhinolophus hipposideros minimus* Heuglin, 1861 and *Myotis* sp. (Shahack-Gross et al., 2004) and inhabited by remarkable blind, undescribed troglobitic species of various taxa: a dysderid spider, palpigrade, pseudoscorpion, mites, isopods and collembola. Although other caves were surveyed in the Karmel

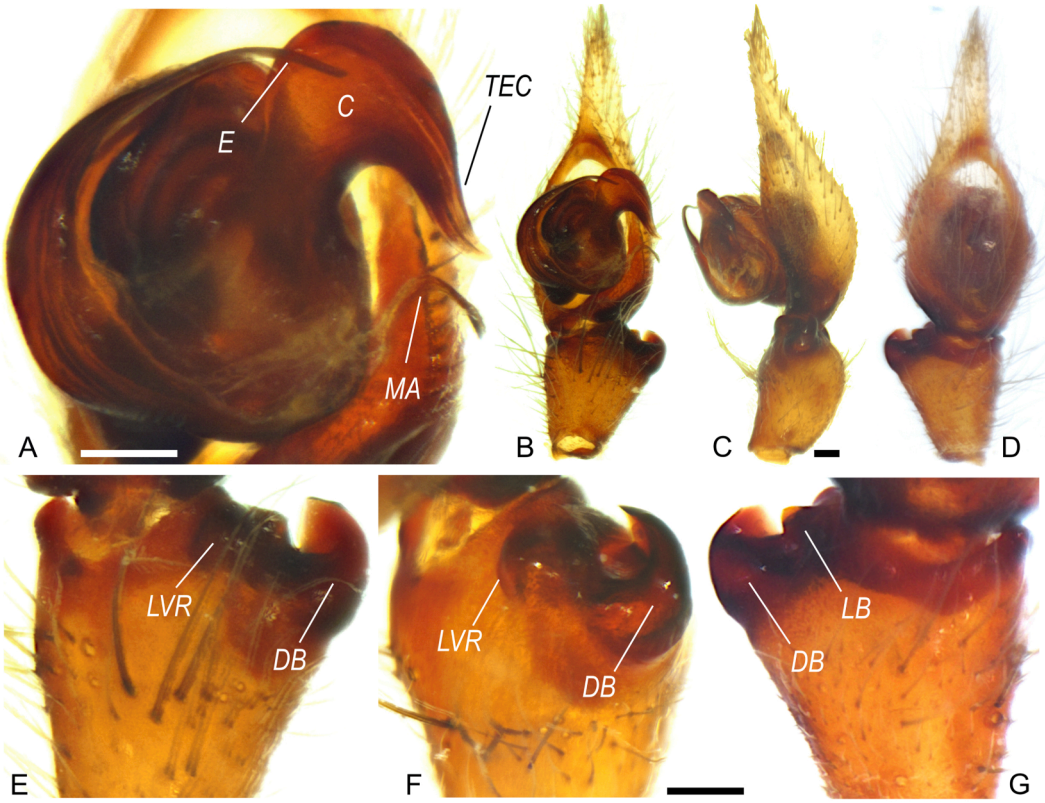

Fig. 15. *Tegenaria naasane* sp. nov., male paratype (HUJ - INVAr 20372). **A-D.** Male left pedipalp, ventral view (**A, B**), retrolateral view (**C**), dorsal view (**D**). **E-G.** Male left pedipalp, RTA in ventral (**E**), retrolateral (**F**) and dorsal views (**G**). *C*, conductor; *DB*, dorsal branch; *E*, embolus; *LB*, lateral branch; *LTR*, lateroventral ridge; *MA*, median apophysis; *TEC*, terminal end of conductor. Scale bars: A-G 0.1 mm.

mountains, Ornit cave is the only locality known for this anophtalmic *Tegenaria* species. During a visit in February 2020, we observed ~ 20 juveniles, two adult females, and two egg sacs placed on the sheet-webs. One adult male, one sub-adult male, several females and and six egg sacs (also placed on the webs) were observed in a survey during August 2022.

Tegenaria naasane sp. nov. Aharon & Gavish-Regev.

LSID:urn:lsid:zoobank.org:act:EBC4CC3F-5D27-4B55-BCA0-7C3BEBFD1A32.

(Figs. 11, 14-15).

Type material

Holotype. **ISRAEL. Judean desert:** A'rak Na'asane cave, 134 m a.s.l., dark zone, (31.9949°N, 35.4074°E), S. Aharon leg., 31/XII/2017, ♀ (HUJ - INVAr 20371).

Paratype. ISRAEL. Judean desert: Same locality and coll. as holotype, 22/XI/2019, 1♂, found dead and dry in a deep section of the cave, (HUJ - INVAr 20372).

Other material examined:

ISRAEL. Judean desert: Same locality as holotype, S. Aharon, G. Gainett, J. Ballesteros, S. Ya'aran leg., 7/VIII/2018, in 96 % ethanol, 1 sub-adult ♀, 1 juvenile (HUJ - INVAr 20373). Same locality, S. Aharon, S. Ya'aran, Y. Aviksis leg., 12/XI/2017, in 96 % ethanol, 3 juveniles (HUJ - INVAr 20374).

Etymology

The species epithet, a noun in apposition, is derived from the name of the cave, which is the type locality of the species. The Arabic name of the cave, Arak Na'asane, means "the cave (or cliff) of the sleepy", is related in the broad sense to an Arab family called Na'asan, who lives in the nearby village, Al Mughayer (B. Langford, personal communication).

Diagnosis

The female of *Tegenaria naasane* sp. nov. differs clearly from all other congeners by 1) inflated and heavily sclerotized median plate laterally. 2) reduced pale region of median plate, forming an elongated and narrow region, rather than wide as in the females of the Israeli troglobitic *Tegenaria* species complex.

The male of *Tegenaria naasane* sp. nov. differs clearly from all other congeners, but share some features with *T. schmalfussi* and the Israeli troglobitic *Tegenaria* species complex *s. lat.* (*T. gainesteros* sp. nov., *T. frumkini* sp. nov., *T. ornit* sp. nov., *T. trogalil* sp. nov. and *T. yaaranford* sp. nov.). No males of *T. yotami* sp. nov. have been found yet. It can be distinguished from all other congeners by the combination of 1) robust and heavily sclerotized RTA, forming a prominent "tilde"-like shape viewed retrolaterally. (Fig. 11), 2) ventral branch of RTA short and thick, fused to the less prominent lateral branch, and to the wide and curved dorsal branch. 3) conductor form a sickle-shaped, terminally pointed as in *T. schmalfussi*, but ends to a slender tip, folded gently on the distal and proximal margins. In the other troglobitic congeners in Israel, the conductor forms a hook-like shape, ends to a short, beak-like shape.

Description

Female (holotype (HUJ - INVAr 20371)):

Coloration. *Carapace* pale yellow, anterior elevated region yellowish to light brown. Frontal area of carapace with middle and anterolaterally light brown regions. *Abdomen* pale yellow. *Colulus* inconspicuous. *Chelicerae* brown. *Labium and Endites* brown. *Sternum* light brown with brown margins. *Legs* yellowish, Coxa of leg I yellow to light brown, femur of pedipalp light brown. *Chelicerae* length 1.76, retromargin teeth 5, promargin teeth 3. *Carapace* length 3.47, width 2.33. *Abdomen:* length 4.08, width 2.91. *Total length* 7.59. *Sternum* length 1.48, width 1.45. *Eye diameters and interdistances* all eyes are absent. **Appendages**. *Pedipalp:* femur 1.67, patella 0.60, tibia 1.14, tarsus 1.50. *Leg I:* femur (fe) 4.58, patella (pa) 1.22, tibia (ti) 4.71, metatarsus (mt) 4.86, tarsus (ta) 2.40. *II:* fe 4.19, pa 1.10, ti 4.09, mt 4.50, ta 1.86. *III:* fe 3.90, pa 1.15, ti 3.60, mt 4.30, ta 1.70. *IV:* fe 4.72, pa 1.02, ti 4.58, mt 5.60, ta 1.93. *Epigynum* length 0.26, width 0.71. Long hairs on ventral side of tarsi I-II. Patella with two dorsal spines but without lateral spines,

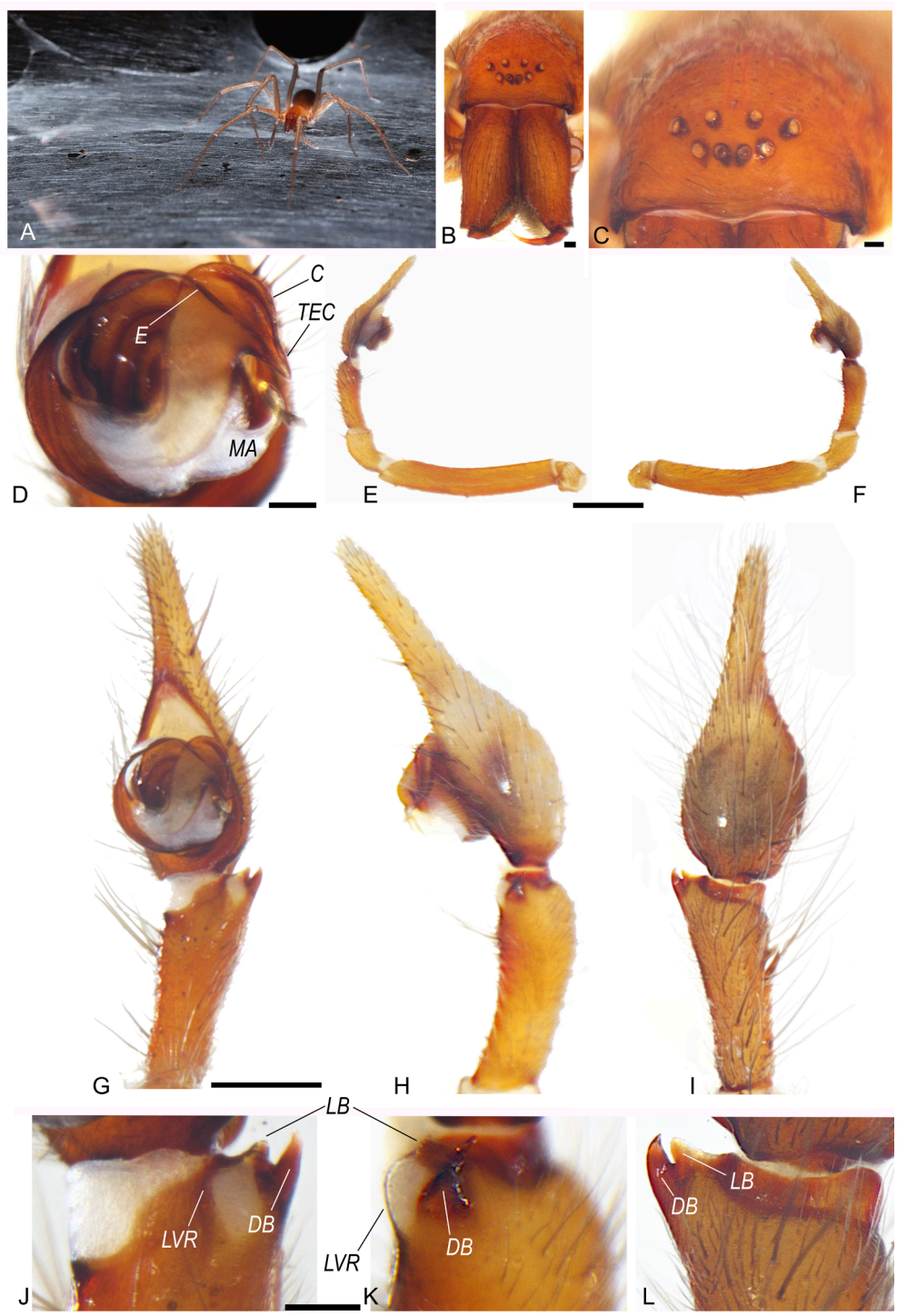

Fig. 16. *Tegenaria frumkini* sp. nov. **A.** Live habitus, Bor Ha'Navi cave, Ofra (Pic. B. Langford). **B-L.** Male holotype (HUJ - INVAr 20399). **B.** Carapace and chelicera, frontal view. **C.** Eyes region, frontal view. **D-I.** Male left pedipalp, ventral view (**D, G**), prolateral view (**E**), retrolateral view (**F, H**), dorsal view (**I**). **J-L.** Male left pedipalp, RTA in ventral (**J**), retrolateral (**K**) and dorsal views (**L**). *C*, conductor; *DB*, dorsal branch; *E*, embolus; *LB*, lateral branch; *LTR*, lateroventral ridge; *MA*, median apophysis; *TEC*, terminal end of conductor. Scale bars: B-D, J-L 0.1 mm; E-F 1 mm; G-I 0.5 mm.

pedipalp patella with 2 dorsal spines and 1 prolateral spine. ventral spines absent on all tarsi. **Epigynum and vulva**. *Median plate* inflated and heavily sclerotized laterally, forming two blackish bulge protruding dorsoventrally. Pale median area between the lateral bulge is narrow and depressed. Epigynum 2.5 wider than long. *Lateral margin* semi sclerotized and somewhat inflated. Copulatory openings form a narrow slit in between the sclerotized margin of the median plate and the lateral margin (see arrows in Fig. 14B-C). *Vulva* was not dissected, but receptacles are somewhat reflected through epigynal plate.

Male (paratype (HUJ - INVAr 20372)):

Coloration. *Carapace* posterior region pale brown, anterior elevated region yellowish to light brown. *Abdomen* missing. *Chelicerae* light brown. *Labium and Endites* brown. *Sternum* yellowish to light brown. *Legs* (only leg I found) proximal half femur of leg I with warm brown to reddish pattern, the rest distal part of femur is pale yellow. *Chelicerae* length 1.45, retromargin teeth 4 or 5, promargin teeth 3. *Carapace* length 2.89, width 2.57. *Sternum* length 1.18, width 1.19. *Eye diameters and interdistances* all eyes are absent. **Appendages**. *Pedipalp:* tibia 0.77, tarsus 1.60. Other legs are missing. **Pedipalp**. *RTA* with three sclerotized branches, lateroventral ridge reduced. Ventral branch short and sclerotized, curved distally, fused dorsally to the less prominent lateral branch, and laterally to the dorsal branch. Dorsal branch prominent,

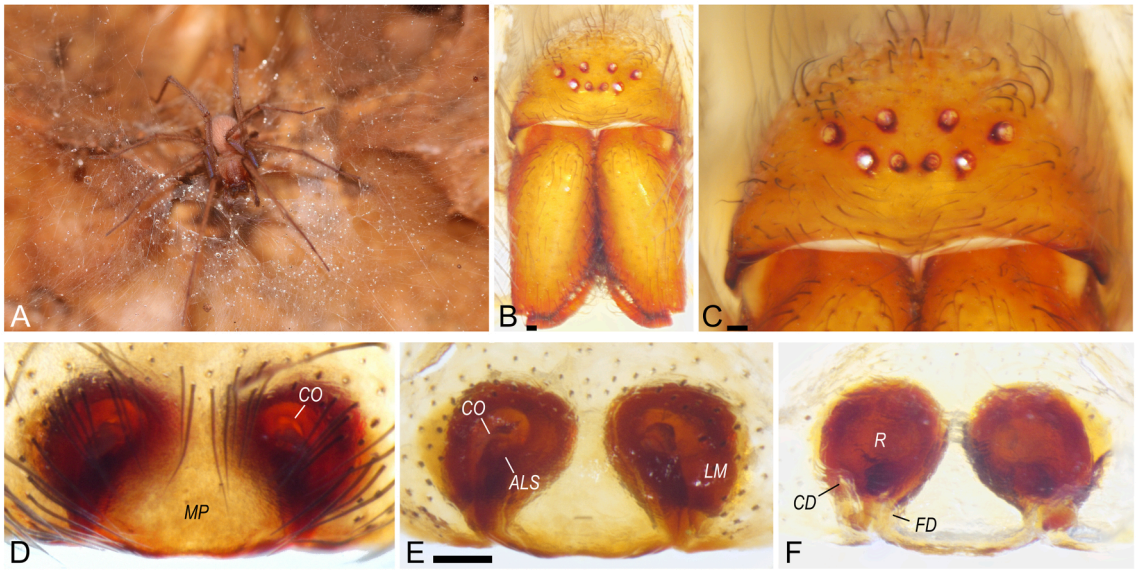

Fig. 17. *Tegenaria frumkini* sp. nov. **A.** Adult female from Neta cave, live habitus. **B-F.** Female paratype. **B.** Carapace and chelicera, frontal view. **C.** Eyes region, frontal view. **D-E.** Epigynum, ventral view, before (**D**) and after (**E**) clearing. **F.** Vulva, dorsal view. *ALS*, anterolateral sclerite of median plate; *CD*, copulatory duct; *CO*, copulatory opening; *FD*, fertilization duct; *LM*, lateral margin of epigynum; *R*, receptaculum. Scale bars: B-F 0.1 mm.

strongly curved dorsally, ending with thin but wide edge. Lateral branch smaller than the other branches, sclerotized. Ventral and dorsal branches forming a "tilde"-like shape viewed retrolaterally. *embolus* moderately long, filiform distally. Originating at 9o'clock position, distal end at 1o'clock position. *conductor* sickle-shaped, rounded distally. Distal and retrolateral margins folded all along to the terminal end of conductor. Terminal end slenderly elongated, pointed and somewhat curved, folded gently at the distal and proximal margins, forming a slender groove along the folding. *MA* membranous, moderately long and narrow. Bent distally, with distal sclerite.

Distribution and natural history

Known only from type locality. *Tegenaria naasane* sp. nov. is a troglobitic species, totally eyeless, missing all ocelli and eye pigmentation. The male was found dead and dry on the cave floor, hence the female was designated as holotype. The spiders were found in a limited area in the deep sections of A'rak Na'asane cave (Z, K in the cave map, see (Frumkin et al., 2018)) which experience a steady temperature of 25.6–25.7 °C and a high relative humidity of 98.1–98.7 %. The inner section of the cave is inhabited by other endemic troglobite arthropods, such as the opilionid *Haasus naasane* Aharon et al. 2019, an undescribed pseudoscorpion and other undescribed hexapods. The rich arthropods assembly, are mostly foraging on the thick layer of guano covering the cave floor, deposited by a colony of hundreds of *Asellia tridens* (É. Geoffroy, 1813) bats, while *T. naasane* sp. nov. were found at the edge of the guano deposition. The cave is located at the border between the semiarid eastern Samaria region and arid northern Judean desert (Frumkin et al., 2018), and it is the largest maze cave in Israel by volume (35,161 m^3) and the third longest limestone cave in Israel (2238 m) (ICRC data, personal communication, 2021).

Tegenaria frumkini sp. nov. Aharon & Gavish-Regev.

LSID:urn:lsid:zoobank.org:act:0BBAB5E5-5C01-44EE-8663-CA21B7FF471B.

(Figs. 11, 16-17).

Type material

Holotype. ISRAEL. Samaria mountains: Ofra, Neta Cave, 827 m a.s.l., dark zone, (31.9596°N, 35.2673°E), S. Aharon, S. Ya'aran, J.A. Ballesteros leg., 8/VIII/2018, ♂ (HUJ - INVAr 20399).

Paratypes. ISRAEL. Samaria mountains: same data as holotype, 2♀ (HUJ - INVAr 20397–20398). Ofra, Nof-Amona cave, 800 m a.s.l., epikarst, (31.9535°N, 35.2691°E), S. Aharon, S. Ya'aran leg., 14/VII/2020, 1♂ (HUJ - INVAr 20338), 1♀ (HUJ - INVAr 20337).

Other material examined:

ISRAEL. Samaria mountains: Same data as holotype, in 96 % ethanol, 2♀♀ (HUJ - INVAr 20419), (HUJ - INVAr 20452), 1♀, 16 juveniles (HUJ - INVAr 20420). Ofra, Capara cave, 821 m a.s.l., dark zone, (31.9593°N, E35.2649°E), S. Aharon, S. Ya'aran, J.A. Ballesteros leg., 8/VIII/2018, in 96 % ethanol, 1♀ (HUJ - INVAr 20395), 1♀, 10 juveniles, 1 sub-adult male (HUJ - INVAr 20396).

Etymology

The species is named in honor of Prof. Amos Frumkin, the founder of the speleological research in Israel and the Israel Cave Research Center (ICRC). Frumkin's hometown, Ofra, is located few hundred meters from Ofra karst basin, which he discovered and studied already at the 1970 s.

Diagnosis

Males of *Tegenaria frumkini* sp. nov. are most similar to the species in the Israeli troglobitic *Tegenaria* species complex *s. lat.* (*T. gainesteros* sp. nov., *T. ornit* sp. nov., *T. naasane* sp. nov., *T. trogalil* sp. nov., *T. yaaranford* sp. nov.) and to *T. schmalfussi*. No males of *T. yotami* sp. nov. have been found yet. The males can be hardly distinguished from *T. gainesteros* sp. nov., *T. trogalil* sp. nov., and *T. yaaranford* sp. nov., but differs from the other congeners by the combination of 1) RTA with a pointed, tusk-like dorsal branch, rather than a blunt edged dorsal branch in *Tegenaria ornit* sp. nov., a robust and heavily sclerotized RTA, forming a "tilde"-like shape in *Tegenaria naasane* sp. nov., and short blunt RTA in *T. schmalfussi.* (Fig. 11), 2) conductor that forms a hook-like shape, ends to a short, beak-like shape, rather than a sickle-shaped, terminally pointed in *T. naasane* sp. nov. and *T. schmalfussi*.

Females are similar to the species in the Israeli troglobitic *Tegenaria* species complex *s. lat.* (except *T. naasane* sp. nov.) and to *T. lazarovi* and *T. ariadnae*. Females can be distinguished from *T. lazarovi* and *T. ariadnae* by 1) broader shape of epigynal median plate rather than anteriorly broad in *T. ariadnae*. 2) copulatory openings forming a crescent-like slit shape, while they are straight and perpendicular to the epigynal median plate in *T. lazarovi* and horizontaly opened in *T. ariadnae*. Females differ from the other Israeli troglobitic species by the combination of 1) pale region of median plate before clearing, forming a sub oval to oval shape, wider posteriorly. 2) semicircular, prominent, and more sclerotized lateral margins, relative to *T. gainesteros* sp. nov., *T. ornit* sp. nov., *T. trogalil* sp. nov., *T. yotami* sp. nov., with copulatory openings small, but visible anteriorly.

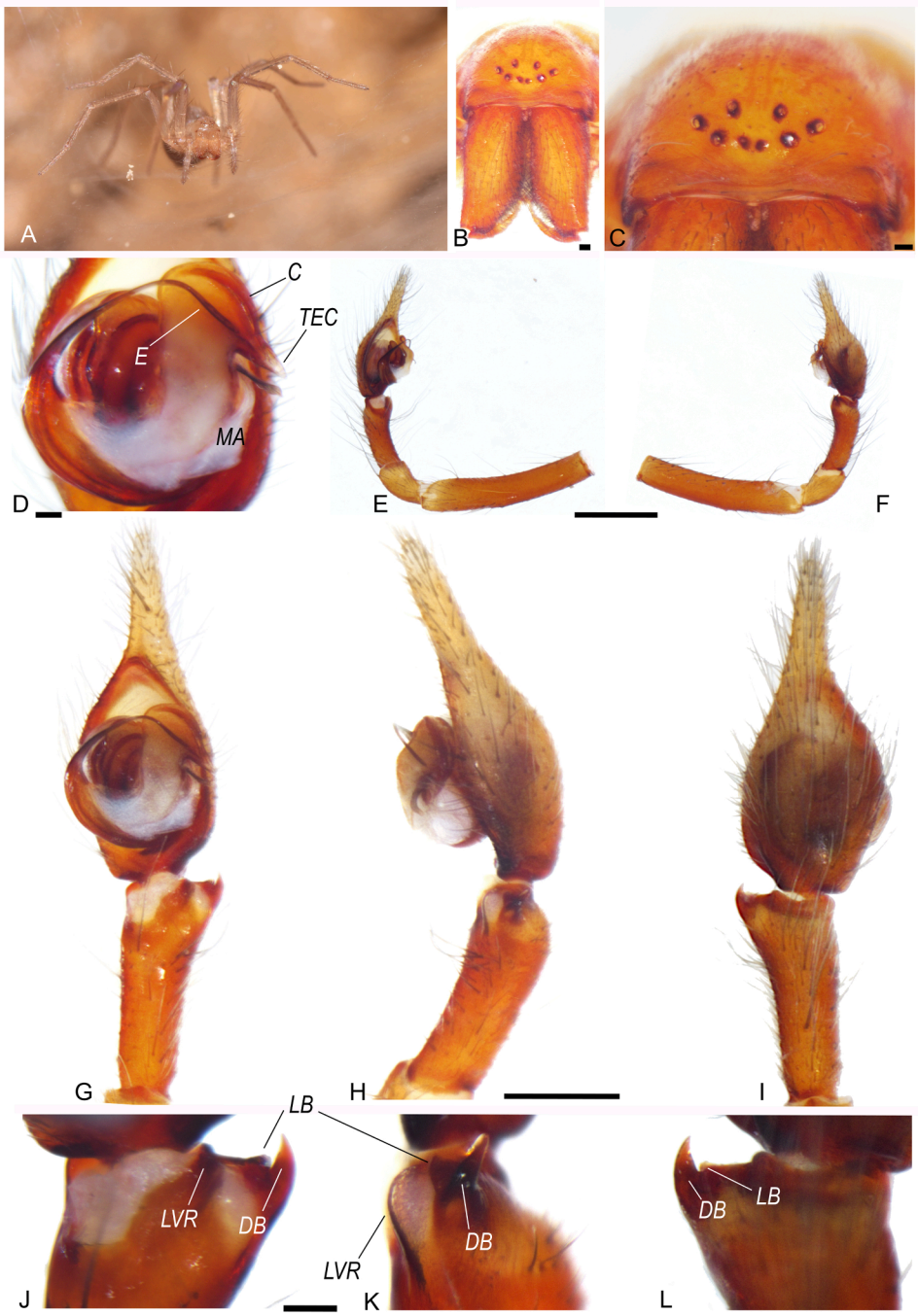

Fig. 18. *Tegenaria gainesteros* sp. nov. **A.** Live habitus, 'En Sarig (water tunnel). **B-L.** Male paratype (HUJ - INVAr 20390). **B.** Carapace and chelicera, frontal view. **C.** Eyes region, frontal view. **D-I.** Male left pedipalp, ventral view (**D, G**), prolateral view (**E**), retrolateral view (**F, H**), dorsal view (**I**). **J-L.** Male left pedipalp, RTA in ventral (**J**), retrolateral (**K**) and dorsal views (**L**). *C*, conductor; *DB*, dorsal branch; *E*, embolus; *LB*, lateral branch; *LTR*, lateroventral ridge; *MA*, median apophysis; *TEC*, terminal end of conductor. Scale bars: B-D, J-L 0.1 mm; E-F 1 mm; G-I 0.5 mm.

Description

Male (holotype (HUJ - INVAr 20399)):

Coloration. *Carapace* posterior region yellowish, anterior elevated region light brown to red brown. *Abdomen* depigmented. *Colulus* inconspicuous. *Chelicerae* reddish brown. *Labium and Endites* brown. *Sternum* warm yellow with brown margins. *Legs* yellowish, femur of legs I-II and pedipalps are warm brown. *Chelicerae* length 1.65, retromargin teeth 5, promargin teeth 3. *Carapace* length 3.75, width 2.95. *Abdomen:* length 4.61, width 2.82. *Total length* 8.36. *Sternum* length 1.46, width 1.40. *Clypeus* length 0.31. *Eye diameters and interdistances* AME 0.09, ALE 0.09, PLE 0.08, PME 0.07, AME-AME 0.05, AME-ALE 0.04, ALE-PLE 0.11, PME-PME 0.19, PME-AME 0.14, PME-PLE 0.14, PME-ALE 0.12. **Appendages**. *Pedipalp:* femur 2.32, patella 0.70, tibia 0.96, tarsus 1.70. *Leg I:* femur (fe) 7.60, patella (pa) 1.63, tibia (ti) 8.85, metatarsus (mt) 8.90, tarsus (ta) 3.48. *II:* fe 6.60, pa 1.52, ti 6.53, mt 7.48, ta 2.90. *III:* fe 5.46, pa 1.29, ti 5.06, mt 6.65, ta 2.53. *IV:* fe 6.90, pa 1.28, ti 6.42, mt 8.98, ta 2.95. **Pedipalp**. *RTA* with three sclerotized branches, Lateroventral ridge present. Ventral branch flat and less prominent, continuing ventrally to a sclerotized lateroventral ridge. Dorsal branch prominent, tusk-like, protruding and pointed dorsodistally. Lateral branch smaller, protruding oppositely to dorsal branch. *embolus* moderately long and filiform. Originating at 9o'clock position, distal end at 2o'clock position. *conductor* hook-like, rounded distally. Distal and retrolateral margins folded all along to the terminal end of conductor. Terminal end pointed, somewhat elongated beak-like shape, folded gently at the distal and proximal margins, forming a slender groove along the folding. *MA* membranous, twisted distally, with distal sclerite somewhat flattened.

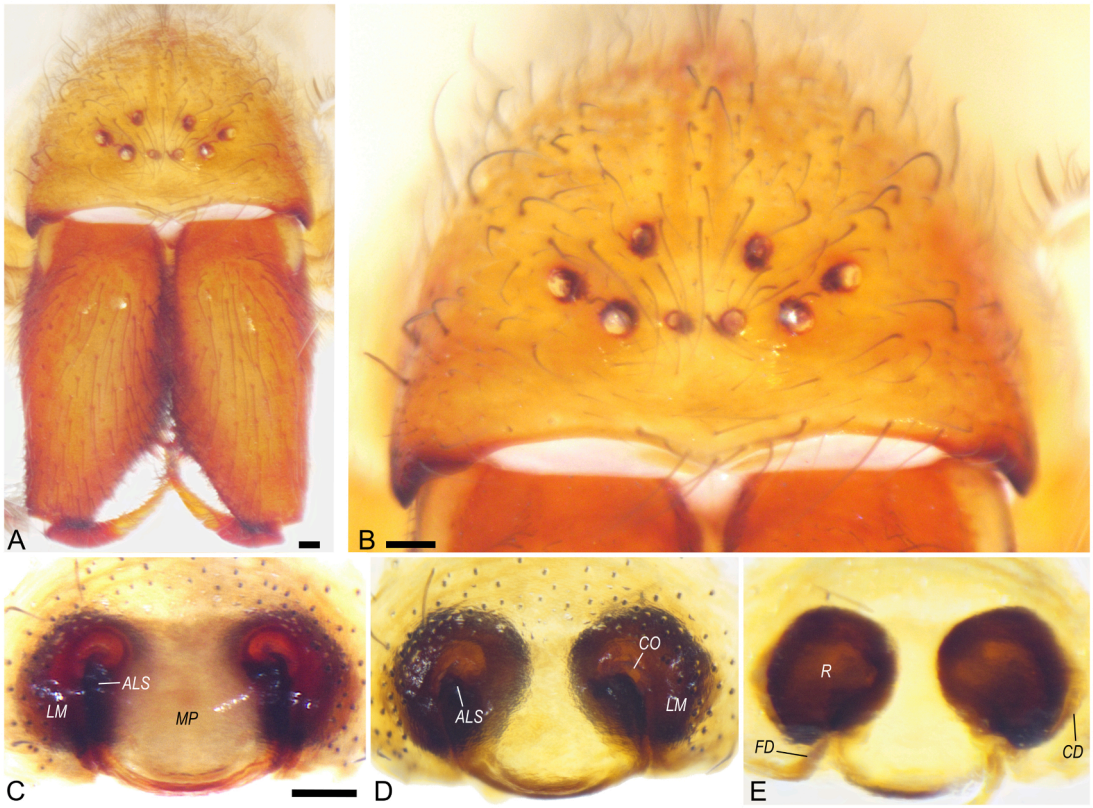

Fig. 19. *Tegenaria gainesteros* sp. nov., female paratype (HUJ - INVAr 20389). **A.** Carapace and chelicera, frontal view. **B.** Eyes region, frontal view. **C-D.** Epigynum, ventral view, before (**C**) and after (**D**) clearing. **E.** Vulva, dorsal view. *ALS*, anterolateral sclerite of median plate; *CD*, copulatory duct; *CO*, copulatory opening; *FD*, fertilization duct; *LM*, lateral margin of epigynum; *R*, receptaculum. Scale bars: B-F 0.1 mm.

Male variation (paratype (HUJ - INVAr20338)):

Coloration. *Carapace* posterior region pale yellow, anterior elevated region light brown. *Abdomen* pale yellow. *Colulus* inconspicuous. *Chelicerae* reddish brown. *Labium and Endites* brown. *Sternum* warm yellow with brown margins. *Legs* yellowish, femur of legs I-II and pedipalps are warm brown. *Chelicerae* length 1.63, retromargin teeth 5, promargin teeth 3. *Carapace* length 3.43, width 2.60. *Abdomen:* length 3.50, width 2.05. *Total length* 6.93. *Sternum* length 1.56, width 1.52. *Clypeus* length 0.26. *Eye diameters and interdistances* AME 0.07, ALE 0.07, PLE 0.07, PME 0.07, AME-AME 0.02, AME-ALE 0.06, ALE-PLE 0.09, PME-PME 0.12, PME-AME 0.12, PME-PLE 0.12, PME-ALE 0.09. **Appendages**. *Pedipalp:* femur 2.07, patella 0.65, tibia 0.85, tarsus 1.48. *Leg I:* femur (fe) 6.24, patella (pa) 1.29, tibia (ti) 6.85, metatarsus (mt) 6.70, tarsus (ta) 3.19. *II:* fe 5.51, pa 1.31, ti 5.40, mt 5.85, ta 2.73. *III:* fe 4.38, pa 0.93, ti 4.26, mt 5.20, ta 2.17. *IV:* fe 5.44, pa 1.23, ti 5.63, mt 7.27, ta 2.71.

Female (paratypes (HUJ - INVAr 20397), (HUJ - INVAr 20337)):

Coloration. *Carapace* posterior region yellowish, anterior elevated region light brown. *Abdomen* pale brown. *Colulus* inconspicuous. *Chelicerae* light brown. *Labium and Endites* brown. *Sternum* yellowish with brown margins. *Legs* yellowish. *Chelicerae* length 1.97–2.01, retromargin teeth 5, promargin teeth 3. *Carapace* length 4.15–4.20, width 3.05–3.22. *Abdomen:* length 5.01–5.76, width 3.02–3.32. *Total length* 9.16–9.96. *Sternum* length 1.92–1.93, width 1.78–1.82. *Clypeus* length 0.31–0.35. *Eye diameters and interdistances* AME 0.07–0.08, ALE 0.07–0.09, PLE 0.08–0.09, PME 0.07–0.08, AME-AME 0.04–0.06, AME-ALE 0.08, ALE-PLE 0.12, PME-PME 0.19–0.20, PME-AME 0.15, PME-PLE 0.16–0.17, PME-ALE 0.14–0.12. **Appendages**. *Pedipalp:* femur 1.85–2.06, patella 0.61–0.67, tibia 1.31–1.43, tarsus 1.85. *Leg I:* femur (fe) 5.77–6.00, patella (pa) 1.49–1.62, tibia (ti) 5.68–6.14, metatarsus (mt) 5.54–6.15, tarsus (ta) 2.74–2.93. *II:* fe 4.93–5.37, pa 1.39–1.44, ti 4.8–4.96, mt 5.0–5.32, ta 2.43–2.44. *III:* fe 4.45–4.90, pa 1.13–1.17, ti 4.13–4.40, mt 5.11–5.45, ta 2.01–2.08. *IV:* fe 5.74–5.80, pa 1.19–1.47, ti 5.45–5.80, mt 6.67–6.70, ta 2.44–2.64. *Epigynum* length 0.21–0.22, width 0.46–0.47. **Epigynum and vulva**. *Median plate* before clearing, with median pale region sub oval shaped, anterolateral sclerites present, somewhat protruding laterally. After clearing, median plate forming rectangular shape with anterolateral sclerites somewhat protruding anteriorly under the translucent layer of the lateral margin. *Lateral margin* sclerotized, semicircular, copulatory opening small but visible anteriorly. After clearing with semi translucent layer somewhat covering the edge of the anterolateral sclerite. Posteriorly somewhat covering in a thin sclerite layer the posteromargins of the median plate. *Vulva* receptacles globular and sclerotized, somewhat narrower posteriolaterally, surrounded retrolaterally by semisclerotized inconspicuous copulatory ducts, fertilization ducts represented by small, leaf-like appendages.

Remarks and general variation

Although the spiders are presenting reduction of eyes, all ocelli are present and not highly reduced or absent as in the other troglobitic species described herein. Ocelli are encircled by dark pigment.

Distribution and natural history

Known from neighboring caves located at the Ofra karst basin, the southernmost karst plateau in the Levant. The basin is located at the top of the central mountain range of Israel, at the transition between Judean and Samaria mountains, with annual mean precipitation of 500 mm (Frumkin et al., 2017). The holokarst basin (lacking surface drainage) is characterized by active karstification in Amminadav formation, including dolines, sinking streams, vadose caves and vertical shafts, with 41 caves known from a studied area of 5 km^2, ranges from 5.5 m, up to 103.5 m deep (Langford et al., 2019). The karst erosion presumably has started to develop during the Upper Eocene and Oligocene, continued to the Miocene and Pleistocene, However, the karst processes are still active at the present dry Holocene (Frumkin, 1993; Frumkin et al.,

2017). The spiders were found at the deep part of the caves, as well as at the transition and twilight zone, corresponding to the epikarst zone, characterized by a developed fracturing bedrock, which presumably enables the troglobitic spiders to disperse across neighboring caves. During a visit on July 14th, 2020, we observed three sub-adult males and a hatchling of an egg sac (not collected). On another visit during July 25th, 2022, we observed few adult males, and a dozen of females with egg sacs kept at the middle of the sheet-web, rather than the hanged ceiling egg sacs of the sympatric *Tegenaria pagana* found at the entrance and twilight zone.

Tegenaria gainesteros sp. nov. Aharon & Gavish-Regev.

LSID:urn:lsid:zoobank.org:act:E362082C-9983-4CC0-AA49-99FCB20C779A.

(Figs. 11, 18-19).

Type material

Holotype. ISRAEL. Judean mountains: 'En Sarig water tunnel, 723 m a.s.l., dark zone, (31.7568°N, 35.1497°E), S. Aharon leg., 24/IX/2021, ♂ (HUJ - INVAr 20443).

Paratypes. ISRAEL. Judean mountains: same locality as holotype, J.A. Ballesteros & G. Gainett leg., 12/VIII/2018, in 96 % ethanol, 1♂ (HUJ - INVAr 20390), 1♀ (HUJ - INVAr 20389).

Other material examined:

ISRAEL. Judean mountains: Same locality as holotype, J.A. Ballesteros & G. Gainett leg., 12/VIII/2018, in 96 % ethanol, 5 juveniles, 1 sub-adult male (HUJ - INVAr 20391). Same locality, S. Aharon & S. Ya'aran leg., 6/VIII/2018, in 96 % ethanol, 4 juveniles (HUJ - INVAr 20441). Same locality, S. Aharon, S. Ya'aran, J.A. Ballesteros, G. Gainett leg., 6/VIII/2018, in 96 % ethanol, 2 juveniles (HUJ - INVAr 20418).

Etymology

The species name is a combination of the surnames of Guilherme Gainett and Jesus A. Ballesteros, who explored the type locality and collected specimens designated as paratypes material from the spring tunnel.

Diagnosis

Males of *Tegenaria gainesteros* sp. nov are most similar to the species in the Israeli troglobitic *Tegenaria* species complex *s. lat.* (*T. frumkini* sp. nov., *T. ornit* sp. nov., *T. naasane* sp. nov., *T. trogalil* sp. nov. *T. yaaranford* sp. nov.), and to *T. schmalfussi*. No males of *T. yotami* sp. nov. have been found yet. The males can be hardly distinguished from *T. frumkini* sp. nov., *T. trogalil* sp. nov., and *T. yaaranford* sp. nov., but differs from the other congeners by the combination of 1) RTA with a pointed, tusk-like dorsal branch, rather than a blunt edged dorsal branch in *Tegenaria ornit* sp. nov., a robust and heavily sclerotized RTA, forming a "tilde"-like shape in *Tegenaria naasane* sp. nov., and short blunt RTA in *T. schmalfussi.* (Fig. 11), 2) conductor that forms a hook-like shape, ends to a short, beak-like shape, rather than a sickle-shaped, terminally pointed in *T. naasane* sp. nov. and *T. schmalfussi*.

Females are similar to the species in the Israeli troglobitic *Tegenaria* species complex *s. lat.* (except *T. naasane* sp. nov.) and to *T. lazarovi* and *T. ariadnae*. Females can be distinguished from *T. lazarovi* and *T. ariadnae* by 1) broader shape of epigynal median plate rather than anteriorly broad in *T. ariadnae*. 2) copulatory openings forming a crescent-like slit shape, while they are straight and perpendicular to the epigynal median plate in *T. lazarovi* and horizontaly opened in *T. ariadnae*. Females differ from the other Israeli troglobitic species by the combination of 1) pale region of median plate before clearing, forming a subglobular region. 2) dark and prominent anterolateral sclerites, somewhat protruding through the translucent anterioral layer of the lateral margins. 3. Lateral margins sclerotized, semicircular, somewhat inflated medially.

Description

Male (holotype (HUJ - INVAr 20443)):

Coloration. *Carapace* posterior region yellowish, anterior elevated region light brown to red brown. *Abdomen* pale yellow. *Colulus* inconspicuous. *Chelicerae* reddish brown. *Labium and Endites* brown. *Sternum* yellowish with light brown margins. *Legs* yellowish, femur of legs I-II and palps are warm brown. *Chelicerae* length 1.33, retromargin teeth 5 or 6, promargin teeth 3. *Carapace* length 3.04, width 2.46. *Abdomen:* length 3.74, width 2.62. *Total length* 6.78. *Sternum* length 1.51, width 1.47. *Clypeus* length 0.22. *Eye diameters and interdistances* AME 0.02, ALE 0.06, PLE 0.05, PME 0.05, AME-AME 0.11, AME-ALE 0.07, ALE-PLE 0.08, PME-PME 0.19, PME-AME 0.14, PME-PLE 0.15, PME-ALE 0.11. **Appendages**. *Pedipalp:* femur 1.90, patella 0.48, tibia 0.76, tarsus 1.40. *leg I:* fe 4.83, pa 1.21, ti 5.11, mt 5.25, ta 2.27. *leg II:* fe 3.96, pa 1.10, ti 4.17, mt 4.30, ta 2.17. *III:* fe 3.51, pa 0.97, ti 3.58, mt 4.26, ta 1.90. *IV:* fe 4.43, pa 0.90, ti 4.50, mt 5.92, ta 2.30. **Pedipalp**. *RTA* with three sclerotized branches. Lateroventral ridge present. Ventral branch flat and less prominent, semisclerotized, continuing ventrally to a sclerotized lateroventral ridge. Dorsal branch prominent, tusk-like, protruding and pointed dorsodistally. Lateral branch smaller, protruding oppositely to dorsal branch. *embolus* moderately long and filiform. Originating at 9o'clock position, distal end at 2o'clock position. *Conductor* hook-like, rounded distally. Distal and retrolateral margins folded all along to the terminal end of conductor. Terminal end pointed, somewhat slender beak-like shape, folded gently at the distal and proximal margins, forming a groove along the folding. *MA* membranous, twisted distally, with distal sclerite somewhat flattened.

Male variation (paratype (HUJ - INVAr 20390)):

Coloration. *Carapace* posterior region pale yellow, anterior elevated region yellowish to light brown. *Abdomen* pale yellow. *Colulus* inconspicuous. *Chelicerae* reddish brown. *Labium and Endites* light brown. *Sternum* yellowish. *Legs* pale yellow. leg I missing, coxa of legs I-II and femur of leg II light brown. Pedipalps brownish. *Chelicerae* length 1.33, retromargin teeth 5, promargin teeth 3. *Carapace* length 3.26, width 2.45. *Abdomen:* length 3.57, width 2.22. *Total length* 6.83. *Sternum* length 1.69, width 1.57. *Clypeus* length 0.25. *Eye diameters and interdistances* AME 0.03, only one ocellus is present, the other with pigmented area only, ALE 0.05, PLE 0.05, PME 0.05, AME-ALE 0.10, ALE-PLE 0.10, PME-PME 0.21, PME-AME 0.16, PME-PLE 0.15, PME-ALE 0.15. **Appendages**. *Pedipalp:* femur 2.03, patella 0.61, tibia 0.76, tarsus 1.53. *leg II:* fe 4.74, pa 1.10, ti 4.13, mt 4.86, ta 2.22. *III:* fe 3.93, pa 0.80, ti 3.70, mt 4.29, ta 2.14. *IV:* fe 4.42, pa 1.02, ti 4.54, mt 6.22, ta 2.38.

Female (paratype (HUJ - INVAr 20389)):

Coloration. *Carapace* posterior region pale yellow, anterior elevated region yellowish to light brown. *Abdomen* pale yellow. *Colulus* inconspicuous. *Chelicerae* reddish brown. *Labium and Endites* light brown. *Sternum* yellowish. *Legs* pale brown, proximal half femur of leg I with warm brown, femur of pedipalp light brown. *Chelicerae* length 1.83, retromargin teeth 5, promargin teeth 3. *Carapace* length 3.67, width 2.80. *Abdomen:* length 4.35, width 2.51. *Total length* 8.02. *Sternum* length 1.86, width 1.74. *Clypeus* length 0.27. *Eye diameters and interdistances* AME 0.04 and 0.06, ALE 0.07, PLE 0.06, PME 0.05, AME-AME 0.11, AME-ALE 0.11, ALE-PLE 0.13, PME-PME 0.28, PME-AME 0.21, PME-PLE 0.21, PME-ALE 0.19. **Appendages**. *Pedipalp:* femur 1.88, patella 0.45, tibia 1.04, tarsus 1.84. *Leg I:* femur (fe) 4.81, patella (pa) 1.51, tibia (ti) 4.85, metatarsus (mt) 5.11, tarsus (ta) 2.36. *II:* fe 4.44, pa 1.13. *III:* fe 2.85, pa 0.82, ti 2.73, mt 3.09, ta 1.44. *IV:* fe 5.00, pa 0.86. *Epigynum* length 0.26, width 0.48. **Epigynum and vulva**. *Median plate* before clearing, with subglobular median pale region, with dark sclerotized anterolateral sclerites. After clearing, median plate forming rectangular shape with anterolateral sclerites protruding dorsally through the translucent anterior layer of the lateral margins. *Lateral margin* sclerotized, semicircular, somewhat inflated medially. With semi translucent layer, kidney shape, somewhat covering the edge of the anterolateral sclerite and the copulatory opening. Posteriorly somewhat covering in a thin sclerite layer the posteromargins of the median plate. *Vulva* receptacles globular and sclerotized, somewhat pointed posteriolaterally, surrounded retrolaterally by semisclerotized inconspicuous copulatory ducts, fertilization ducts small, leaf-like appendages.

Remarks and general variation

Usually all eight eyes are present, encircled by reddish to dark pigment. AME are more reduced than other eyes, sometimes one or two

Fig. 20. *Tegenaria yaaranford* sp. nov. **A.** Live habitus, sub-adult male feeding on a fly, Te'omim cave. **B-L.** Male paratype (HUJ - INVAr 20442). **B.** Carapace and chelicera, frontal view. **C.** Eyes region, frontal view. **D-I.** Male left pedipalp, ventral view (**D, G**), prolateral view (**E**), retrolateral view (**F, H**), dorsal view (**I**). **J-L.** Male left pedipalp, RTA in ventral (**J**), retrolateral (**K**) and dorsal views (**L**). *C*, conductor; *DB*, dorsal branch; *E*, embolus; *LB*, lateral branch; *LTR*, lateroventral ridge; *MA*, median apophysis; *TEC*, terminal end of conductor. Scale bars: B-D, J-L 0.1 mm; E-F 1 mm; G-I 0.5 mm.

AME ocelli absent, with residual red pigment in the ocellus position.

Distribution and natural history

Known only from the type locality. *Tegenaria gainesteros* sp. nov. is a troglobitic species, found in the spring tunnel of 'En Sarig. The spring flows in between the karstified Amminadav formation, and the aquiclude Motza formation. This ancient spring tunnel (Hebrew: Niqba'), is based on a perched spring, excavated sub-horizontally deep into the karstic rock at the base of the spring (Yechezkel and Frumkin, 2016). *T. gainesteros* sp. nov. was collected mainly at the dark section, while the sympatric *Tegenaria dalmatica* species was collected at the entrance and along the excavated tunnel. Since many spring tunnels are present at the Judean mountains, it is most likely to find more troglobitic *Tegenaria* morphospecies at similar habitats.

Tegenaria yaaranford sp. nov. Aharon & Gavish-Regev.

LSID:urn:lsid:zoobank.org:act:4EE20513-2E77-4613-A5C5-FF7B52BFC324.

(Figs. 11, 20-21).

Type material

Holotype. ISRAEL. Judean mountains: Te'omim cave, 405 m a.s.l., transition zone, (31.7262°N, 35.0217°E), S. Aharon leg., 12/IX/2021, ♂

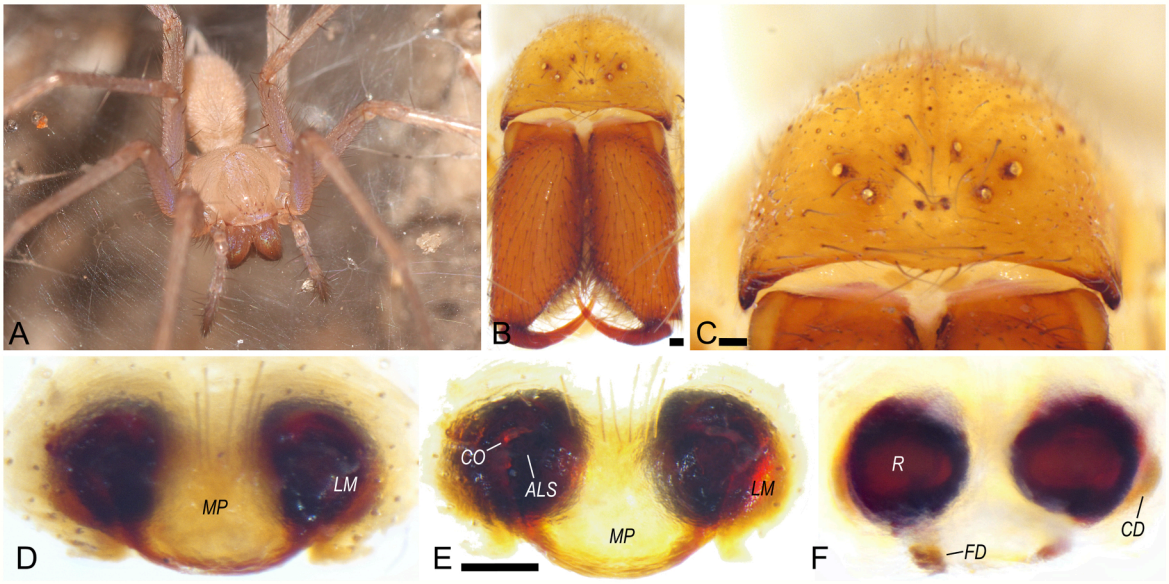

Fig. 21. *Tegenaria yaaranford* sp. nov. **A.** Live habitus. **B-F.** Female paratype (HUJ - INVAr 20358). **B.** Carapace and chelicera, frontal view. **C.** Eyes region, frontal view (notice highly reduced eyes, AME ocelli absent, only residual pigment present). **D-E.** Epigynum, ventral view, before (**D**) and after (**E**) clearing. **F.** Vulva, dorsal view. *ALS*, anterolateral sclerite of median plate; *CD*, copulatory duct; *CO*, copulatory opening; *FD*, fertilization duct; *LM*, lateral margin of epigynum; *R*, receptaculum. Scale bars: B-F 0.1 mm.

(HUJ - INVAr 20445).

Paratypes. ISRAEL. Judean mountains: Same data as holotype, 1♀ (HUJ - INVAr 20446). Same locality, dark zone, S. Aharon & E. Gavish-Regev leg., 3/X/2017, 1♂ (HUJ - INVAr 20442). Same locality, S. Aharon & E. Gavish-Regev leg., 31/III/2014, 3♀ (HUJ - INVAr 20358), (HUJ - INVAr 20359), (HUJ - INVAr 20360).

Other material examined:

ISRAEL. Judean mountains: Same locality as holotype, S. Aharon, E. Gavish-Regev, P.P. Sharma, G. Gainett, J.A. Ballesteros, I. Armiach-steinpress leg., 23/VII/2018, 1♂ (HUJ - INVAr 20356), 1♀ (HUJ - INVAr 20357). Same data, in 96 % ethanol, 1♀ (HUJ - INVAr 20392), 2 sub-adult males (HUJ - INVAr 20417). Same locality, S. Aharon & E. Gavish-Regev leg., 3/X/2017, 1 juvenile, 1 sub-adult male (HUJ - INVAr 20440).

Etymology

The species name is a combination of the surnames of Boaz Langford and Shemesh Ya'aran, both keen geologists and speleologists who are contributing to Israel cave research. In Te'omim cave, the type locality of this species, S. Ya'aran took part in revealing rich assemblage of oil-lamps from the Late Roman period in the cave (Zissu et al., 2011a), while B. Langford discovered outstanding hoard and remains of Bar Kokhba Revolt including weapons and rare coins (Zissu et al., 2011b).

Diagnosis

Males of *Tegenaria yaaranford* sp. nov. are most similar to the species in the Israeli troglobitic *Tegenaria* species complex *s. lat.* (*T. frumkini* sp. nov., *T. gainesteros* sp. nov., *T. ornit* sp. nov., *T. naasane* sp. nov., *T. trogalil* sp. nov.), and to *T. schmalfussi*. No males of *T. yotami* sp. nov. have been found yet. The males can be hardly distinguished from *T. gainesteros* sp. nov., *T. frumkini* sp. nov. and *T. trogalil* sp. nov., but differs from the other congeners by the combination of 1) RTA with a pointed, tusk-like dorsal branch, rather than a blunt edged dorsal branch in *Tegenaria ornit* sp. nov., a robust and heavily sclerotized RTA, forming a "tilde"-like shape in *Tegenaria naasane* sp. nov., and short blunt RTA in *T. schmalfussi.* (Fig. 11), 2) conductor forms a hook-like shape, ends to a short, beak-like shape, rather than a sickle-shaped, terminally pointed in *T. naasane* sp. nov. and *T. schmalfussi.*

Females are similar to the species in the Israeli troglobitic *Tegenaria* species complex *s. lat.* (except *T. naasane* sp. nov.) and to *T. lazarovi* and *T. ariadnae*. Females can be distinguished from *T. lazarovi* and *T. ariadnae* by 1) broader shape of epigynal median plate rather than anteriorly broad in *T. ariadnae*. 2) copulatory openings forming a crescent-like slit shape, while they are straight and perpendicular to the epigynal median plate in *T. lazarovi* and horizontaly opened in *T. ariadnae*. Females differ from the other Israeli troglobitic species by the following characters. 1) pale region of median plate before clearing, forming a trapezoidal shape, longer than wide. 2) median plate forming a semicircular or shovel-like shape after clearing, with prominent and heavy sclerotized anterolateral sclerite.

Description

Male (holotype (HUJ - INVAr 20445)):

Coloration. *Carapace* posterior region pale brown, anterior elevated region light brown. *Abdomen* pale yellow. *Colulus* inconspicuous. *Chelicerae* light brown. *Labium and Endites* light brown. *Sternum* pale with yellow margins. *Legs* pale brown, palp and proximal half femur I brown, proximal half of femur II light brown. *Chelicerae* length 1.33, retromargin teeth 5, promargin teeth 3. *Carapace* length 2.92, width 2.35. *Abdomen:* length 3.25, width 1.73. *Total length* 6.17. *Sternum* length 1.47, width 1.40. *Clypeus* length 0.23. *Eye diameters and interdistances* AME ocelli are absent, diameter of the pigmented area is 0.03, ALE 0.04, PLE 0.04, PME 0.02, ALE-PLE 0.12, PME-PME 0.22, PME-PLE 0.17, PME-ALE 0.17. **Appendages**. *Pedipalp:* femur 1.97, patella 0.56, tibia 0.80, tarsus 1.40. *Leg I:* femur (fe) 4.88, patella (pa) 1.12, tibia (ti) 5.07, metatarsus (mt) 5.2, tarsus (ta) 2.61. *II:* fe 4.4, pa 0.97, ti 4.16, mt 4.69, ta 2.32. *III:* fe 3.96, pa 1.07, ti 3.35, mt 4.48, ta 1.81. *IV:* fe 4.92, pa 1.07, ti 4.63, mt 6.03, ta 2.12. Relatively long hairs on ventral side of tarsi I-II. **Pedipalp**. *RTA* with three sclerotized branches, Lateroventral ridge present. Ventral branch flat and less prominent, semisclerotized, continuing ventrally to a sclerotized lateroventral ridge. Dorsal branch prominent, tusk-like, protruding and pointed dorsodistally. Lateral branch smaller, protruding oppositely to dorsal branch. *Embolus* moderately long and filiform. Originating at 9o'clock position, distal end at 2o'clock position. *Conductor* hook-like, rounded distally. Distal and retrolateral margins folded all along to the terminal end of conductor. Terminal end pointed, short beak-like shape, folded gently at the distal and proximal margins, forming a slender groove along the folding. *MA* membranous, twisted distally, with distal sclerite somewhat flattened.

Male variation (paratype (HUJ – INVAr 20442)):

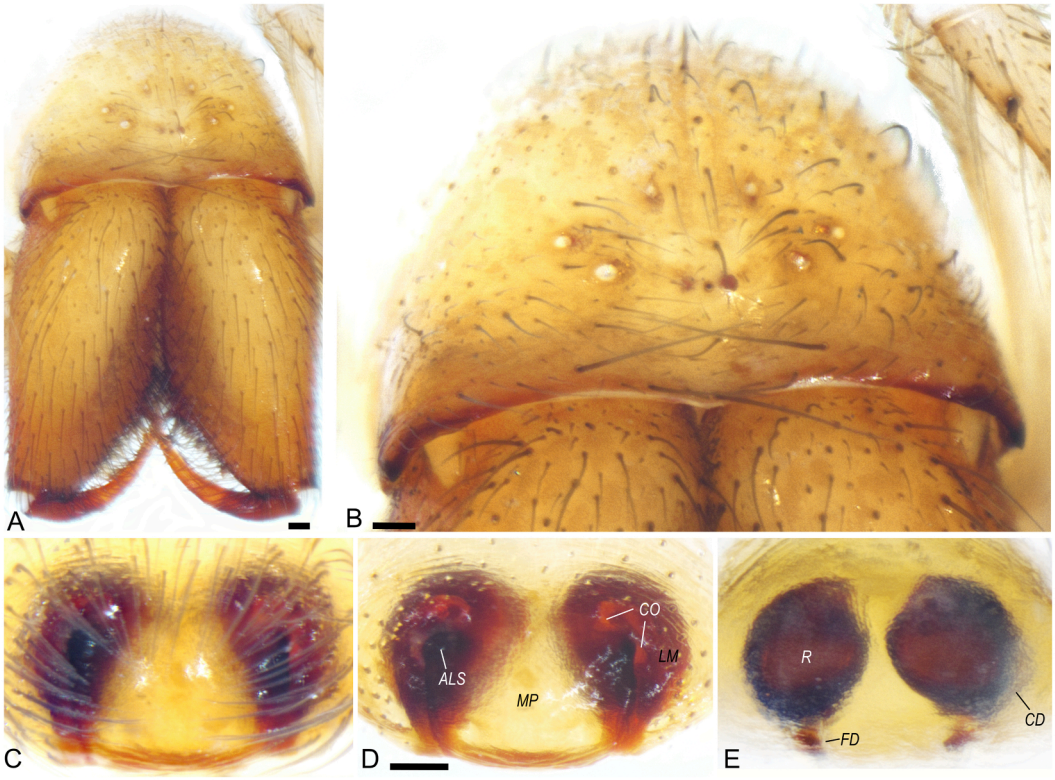

Fig. 22. *Tegenaria yotami* sp. nov., female paratype (HUJ - INVAr 20385). **A.** Carapace and chelicera, frontal view. **B.** Eyes region, frontal view (notice highly reduced eyes, AME ocelli absent, only residual pigment present). **C-D.** Epigynum, ventral view, before (**C**) and after (**D**) clearing. **E.** Vulva, dorsal view. *ALS*, anterolateral sclerite of median plate; *CD*, copulatory duct; *CO*, copulatory opening; *FD*, fertilization duct; *LM*, lateral margin of epigynum; *R*, receptaculum. Scale bars: B-F 0.1 mm.

Coloration. *Carapace* posterior region pale yellow, anterior elevated region yellowish to light brown. *Abdomen* pale yellow. *Colulus* inconspicuous. *Chelicerae* yellowish to light brown. *Labium and Endites* light brown. *Sternum* pale with yellow margins. *Legs* pale brown, Coxa of leg I yellow to light brown, femur of pedipalp light brown. *Chelicerae* length 1.33, retromargin teeth 6, promargin teeth 3. *Carapace* length 2.74, width 2.18. *Abdomen:* length 3.42, width 2.28. *Total length* 6.16. *Sternum* length 1.42, width 1.35. *Clypeus* length 0.20. *Eye diameters and interdistances* AME ocelli are absent, diameter of the pigmented area is 0.04, ALE 0.06, PLE 0.05, PME 0.03, ALE-PLE 0.12, PME-PME 0.16, PME-PLE 0.20, PME-ALE 0.15. **Appendages**. *Pedipalp:* femur 1.84, patella 0.53, tibia 0.75, tarsus 1.40. *Leg I:* femur (fe) 4.50, patella (pa) 0.80, tibia (ti) 4.44, metatarsus (mt) 4.68, tarsus (ta) 2.46. *II:* fe 3.64, pa 0.87, ti 4.06, mt 4.16, ta 2.10. *III:* fe 3.42, pa 0.87, ti 3.62, mt 4.31, ta 1.81. *IV:* fe 3.94, pa 0.97, ti 4.48, mt 5.61, ta 2.09. Long hairs on ventral side of tarsi I-II. Other males show brown-reddish femur I-II.

Female (paratypes)HUJ - INVAr 20358(,)HUJ - INVAr 20446():

Coloration. *Carapace* posterior region pale yellow, anterior elevated region yellowish to light brown. *Abdomen* pale yellow. *Colulus* inconspicuous. *Chelicerae* light brown. *Labium and Endites* light brown. *Sternum* pale with light yellow margins. *Legs* yellowish, femur of pedipalp light brown. *Chelicerae* length 1.76–1.96, retromargin teeth 5 or 6, promargin teeth 3. *Carapace* length 2.02–4.07, width 1.42–2.81. *Abdomen:* length 2.36–4.49, width 1.53–3.20. *Total length* 4.38–8.56. *Sternum* length 1.52–1.76, width 1.43–1.66. *Clypeus* length 0.18–0.28. *Eye diameters and interdistances* AME usually highly reduced or absent. One female with one ocellus present 0.04, the other with pigmented area only, ALE −0.05–0.06, PLE 0.05–0.06, PME 0.03–0.04, AME-ALE 0.16 when one ocellus present, ALE-PLE 0.14–0.18, PME-PME 0.22–0.24, PME-AME 0.22 when one ocellus present, PME-PLE 0.26, PME-ALE −0.24–0.25. **Appendages**. *Pedipalp:* femur 1.83–1.94, patella 0.58–0.65, tibia 1.07–1.18, tarsus 1.57–1.67. *Leg I:* femur (fe) 4.50–5.09, patella (pa) 1.19–1.36, tibia (ti) 4.46–5.23, metatarsus (mt) 4.30–4.88, tarsus (ta) 2.33–2.37. *II:* fe 3.80–4.74, pa 1.10–1.27, ti 3.81–4.6, mt 4.17–4.72, ta 2.03–2.19. *III:* fe 3.97–4.43, pa 1.10–1.15, ti 3.45–4.01, mt 4.30–4.66, ta 1.80. *IV:* fe 4.70–5.42, pa 1.00–1.19, ti 4.64–5.18, mt 5.50–6.15, ta 2.12–2.26. *Epigynum* length 0.23–0.24, width 0.44–0.51. **Epigynum and vulva**. *Median plate* before clearing, with median pale region trapezoidal shaped, longer than wide. Anterolateral sclerite heavily sclerotized, somewhat depressed, forming a semicircular or shovel-like median plate, almost as wide as long. *Lateral margin* sclerotized, semicircular, forming a copulatory opening depression, covered by the anterolateral sclerite of median plate. Posteriorly edging the median plate. *Vulva* receptacles globular and sclerotized, surrounded retrolaterally by semisclerotized copulatory ducts, fertilization ducts represented by small, leaf-like appendages.

Remarks and general variation

All specimens show highly reduced eyes. AME usually absent with residual red pigment. PME sometimes reduced to a slit-like shape. Eyes encircled by fine red pigment.

Distribution and natural history

Known only from the type locality. Te'omim cave, an isolated karst cave, located in the western slope of the Judean mountains, is an hypogenic cave, formed below the water table in dolomitic limestone of the Cenomanian (late Cretaceous) in Weradim Formation (Frumkin et al., 2014; Frumkin and Fischhendler, 2005). Similar caves in similar geological context are Soreq cave (see hereafter) and Shimshon cave (not visited), located 3.5–4.2 north of Te'omim cave (Zissu et al., 2011a). The cave entrance was exposed probably during the end of Pleistocene, but it is likely that cracks and crevices were used by arthropods to enter the cave long before. The cave comprises a large hall (approximately 50 × 70 m) and a narrow side section, the large hall is dominantly inhabited by the frugivorous bat *Rousettus aegyptiacus*, which its guano deposition covers the cave floor. *Tegenaria yaaranford*

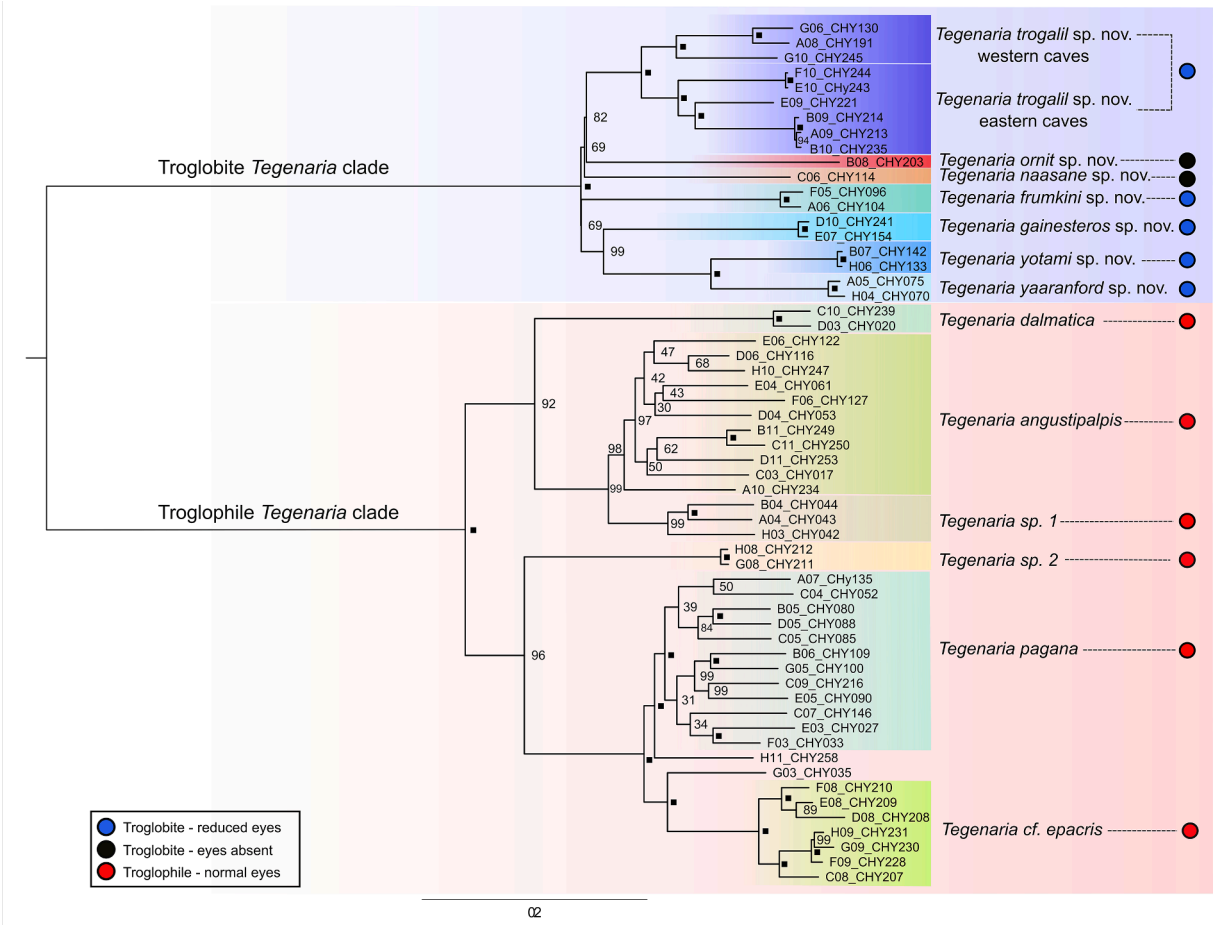

Fig. A1. Maximum likelihood inference of reduced eyes (blue dots) and eyeless (black dots) *Tegenaria* present at the deep sections of the caves and eye-bearing *Tegenaria* present at cave entrance (red dots), based on SNP dataset (untrimmed data). Numbers at nodes represent 1000 bootstrap support. Black squares indicate fully supported clades.

sp. nov. spiders were found at the twilight and dark zone of the cave, with an observation of preying on a moderately large fly, and egg sac kept at the middle of the sub-horizontal sheet-web, rather than the hanged ceiling egg sacs of the sympatric *Tegenaria pagana* found at the entrance and twilight zone.

Tegenaria yotami sp. nov. Gavish-Regev & Aharon.

LSID:urn:lsid:zoobank.org:act:E39F27C5-BAEA-429E-BBCF-835532A2C413.

(Fig. 22).

Type material

Holotype. ISRAEL. Judean mountains: Soreq cave, 405 m a.s.l., (31.7560°N, 35.0227°E), Y. Regev, J.A. Ballesteros, G. Gainett, P.P. Sharma, S. Aharon, E. Gavish-Regev leg., 30/XIII/2018, in 96 % ethanol, ♀ (HUJ - INVAr 20393).

Paratype. ISRAEL. Judean mountains: Same data as holotype, in 96 % ethanol, 1♀ (HUJ - INVAr 20385).

Other material examined:

ISRAEL. Judean mountains: Same data as holotype, in 96 % ethanol, 1♀ (HUJ - INVAr 20416), 1♀, 1 juvenile (HUJ - INVAr 20394).

Etymology

The species is dedicated to Yotam Regev, the husband of the paper's last author (E.G.-R.), who has collected the holotype specimen, and supports E.G-R. arachnological research.

Diagnosis

Females of *Tegenaria yotami* sp. nov. are similar to the other species in the Israeli troglobitic *Tegenaria* species complex *s. lat.* (except *T. naasane* sp. nov.) and to *T. lazarovi* and *T. ariadnae*. Females can be distinguished from *T. lazarovi* and *T. ariadnae* by 1) broader shape of epigynal median plate rather than anteriorly broad in *T. ariadnae*. 2) copulatory openings forming a crescent-like slit shape, somewhat covered by the anterolateral sclerite and laterolateral margins of the median plate, while they are straight and perpendicular to the epigynal median plate in *T. lazarovi* and horizontaly opened in *T. ariadnae*. Females differ from the other Israeli troglobitic species by the combination of 1) pale region of median plate before clearing, forming a trapezoidal shape, longer than wide as in *Tegenaria yaaranford* sp. nov. but with more elongated and narrower lateral margins, longer than wide. 2) median plate forming a rectangular shape after clearing, wider than long. With anterolateral sclerite somewhat covered by semi translucent layer of the lateral margin. No males have been found yet.

Description

Female (holotype (HUJ - INVAr 20393)):

Coloration. *Carapace* pale yellow with yellowish to light brown in anterior elevated region. *Abdomen* pale yellow. *Colulus* inconspicuous. *Chelicerae* light brown. *Labium and Endites* light brown. *Sternum* yellowish with light brown margins. *Legs* pale to light yellow, femur of pedipalp light brown. *Chelicerae* length 1.71, retromargin teeth 5, promargin teeth 3. *Carapace* length 3.08, width 2.38. *Abdomen:* length 3.78, width 2.84. *Total length* 6.86. *Sternum* length 1.61, width 1.37. *Clypeus* length 0.36. *Eye diameters and interdistances* AME ocelli are absent, only some red pigmented spot, ALE 0.05, PLE 0.06, PME 0.04, ALE-PLE 0.12, PME-PME 0.26, PME-PLE 0.21, PME-ALE 0.21. **Appendages**. *Pedipalp:* femur 1.70, patella 0.58, tibia 1.02, tarsus 1.48. *Leg I:* femur (fe) 4.85, patella (pa) 1.36, tibia (ti) 4.98, metatarsus (mt) 4.99, tarsus (ta) 2.45. *II:* fe 4.20, pa 1.22, ti 3.98, mt 3.85, ta 1.82. *III:* fe 3.81, pa 0.94, ti 3.61, mt 4.20, ta 1.81. *IV:* fe 4.63, pa 1.19, ti 4.68, mt 6.18, ta 2.15. *Epigynum*

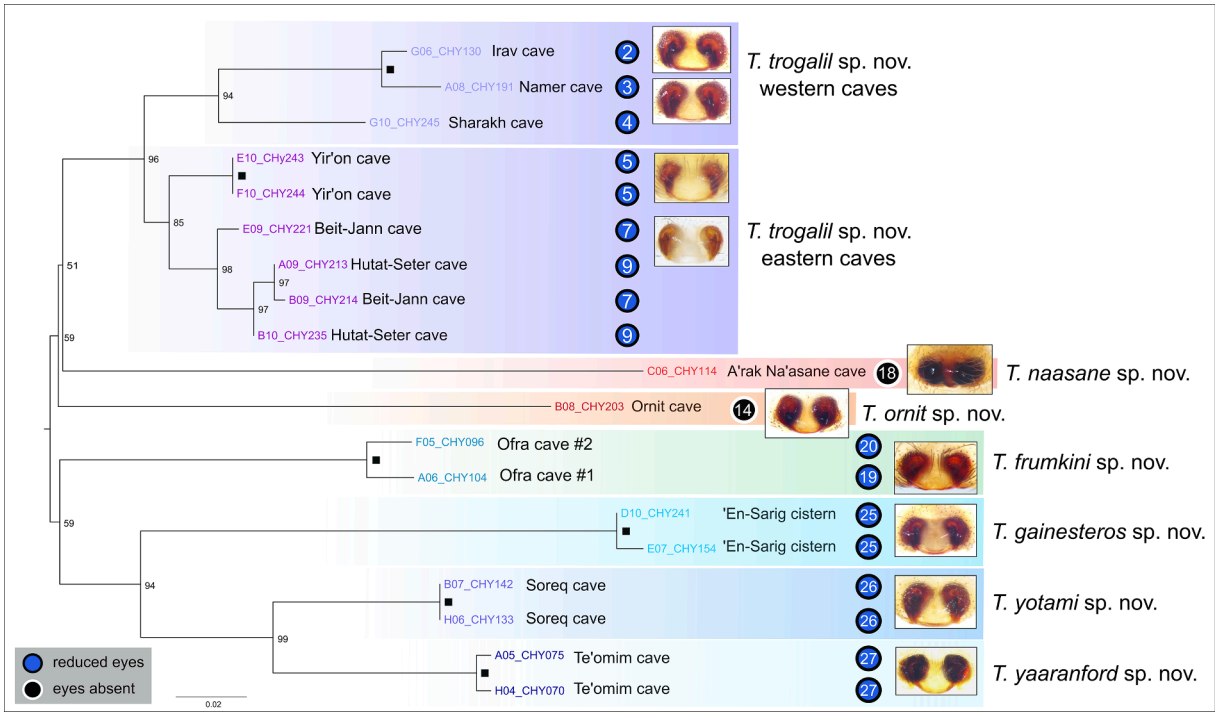

Fig. A2. Maximum likelihood inference of 19 samples of the troglobitic (eyeless and reduced eyes) *Tegenaria* present at the deep section of the caves, based on SNP dataset (10% missing data). Numbers at nodes represent 1000 bootstrap support. Black squares indicate fully supported clades.

length 0.24, width 0.40. **Epigynum and vulva**. *Median plate* before clearing, with median pale region trapezoidal shaped, wider posteriorly. After clearing, median plate forming rectangular shape with antero-lateral sclerites. *Lateral margin* sclerotized, ear-like shaped, longer than wide. Semicircular region anteriorly, with semi translucent layer somewhat covering the edge of the anterolateral sclerite and the copulatory opening. Posteriorly somewhat covering in a thin sclerite layer the posteromargins of the median plate. *Vulva* receptacles globular and sclerotized, slightly pointed anteriorly, copulatory ducts not prominent, fertilization ducts represented by small, leaf-like appendages.

Female (paratype (HUJ - INVAr 20385), (HUJ - INVAr 20394), (HUJ - INVAr 20416)):

Coloration. *Carapace* pale yellow with yellowish to light brown in anterior elevated region. *Abdomen* pale yellow. *Colulus* inconspicuous. *Chelicerae* yellowish to light brown. *Labium and Endites* light brown. *Sternum* yellowish with light brown margins. *Legs* pale to light yellow, femur of pedipalp light brown. *Chelicerae* length 1.2–1.59, retromargin teeth 5, promargin teeth 3. *Carapace* length 2.34–3.05, width 1.73–2.42. *Abdomen:* length 2.53–2.96, width 1.73–2.26. *Total length* 4.87–6.06. *Sternum* length 1.10–1.55, width 1.08–1.49. *Clypeus* length 0.17–0.27. *Eye diameters and interdistances* AME ocelli are absent, only some red pigmented spot, ALE 0.02–0.05, PLE 0.01–0.06, PME 0.02–0.03, ALE-PLE 0.08–0.17, PME-PME 0.16–0.21, PME-PLE 0.15–0.21, PME-ALE 0.13–0.19. **Appendages**. *Pedipalp:* femur 1.2–1.57, patella 0.42–0.59, tibia 0.82–1.10, tarsus 1.02–1.51. *Leg I:* femur (fe) 3.08–4.08, patella (pa) 0.87–1.08, tibia (ti) 3.15–4.46, metatarsus (mt) 3.19–4.51, tarsus (ta) 1.83–2.36. *II:* fe 2.66–3.68, pa 0.85–1.16, ti 2.40–3.79, mt 2.81–4.23, ta 1.32–2.00. *III:* fe 2.66–3.66, pa 0.68–1.12, ti 2.37–3.20, mt 2.77–3.88, ta 1.35–1.78. *IV:* fe 3.32–4.09, pa 0.83–1.05, ti 3.28–4.54, mt 3.98–5.70, ta 1.59–2.21. *Epigynum* length 0.16–0.23, width 0.35–0.40.

Remarks and general variation

All specimens with highly reduced eyes, some with extremely reduced to barely noticed ocelli. AME usually absent, with residual fine pigment. No pigmentation around ocelli.

Distribution and natural history

Known only from the type locality. *Tegenaria yotami* sp. nov. is a troglobitic spider, with highly reduced eyes, lacking the anterior median eyes. The spiders are inhabiting the dark and isolated Soreq cave, located in the western slope of the Judean mountains, and formed at the dolomitic limestone of the Cenomanian (late Cretaceous) in Weradim Formation. The cave comprises a large hall (approximately 60 × 80 m), rich in stalactites, stalagmites and ponds, discovered in 1968 while quiring using explosives. Today, Soreq cave is open to tourists although the nature reserve authorities are doing effort to close the cave tightly between visits. The cave is important for valuable paleoclimate data inferred by Bar-Matthews (Bar-Matthews et al., 1999) and others, analyzing the stable isotopes deposition in speleothems. (see Fig. A1, Fig. A2.)

CRediT authorship contribution statement

Shlomi Aharon: Conceptualization, Investigation, Formal analysis, Writing – original draft. **Jesús A. Ballesteros:** Investigation, Formal analysis, Writing – original draft. **Guilherme Gainett:** Investigation, Writing – review & editing. **Dror Hawlena:** Writing – review & editing, Supervision. **Prashant P. Sharma:** Investigation, Funding acquisition, Writing – review & editing. **Efrat Gavish-Regev:** Conceptualization, Investigation, Supervision, Funding acquisition, Writing – original draft.

Declaration of Competing Interest

The authors declare that they have no known competing financial interests or personal relationships that could have appeared to influence the work reported in this paper.

Acknowledgements

Specimens of *Tegenaria* were collected under permits 2013/40027, 2013/40085, 2014/40313, 2017/41718, 2020/42450, and 2022/43117 from the Israel Nature and Parks Authority to Efrat Gavish-Regev. We thank the Israel Cave Research Center (ICRC), and especially A. Frumkin, S. Ya'aran, B. Langford, A. Cooper, and E. Cohen, and The

Israel National Arachnid Collection staff, and especially, Z. Ganem, S. Warburg, M. Cohen, Y. Zaltz, I. Armiach-Steinpress, Y. Zvik, E. Zvik, R. Shtuhin and A. Uzan, as well as Y. Lubin, I.L.F. Magalhaes, M. Arnedo, N. Berner-Aharon, S. Kulkarni, B. Klementz, H. Steiner for assistance in the field and valuable discussions.

Special thanks for N. Achituv, for drawings used in Fig. 6 and graphical abstract, and B. Langford for picture used in the graphical abstract. Sequencing was performed at the at CD Genomics. Access to computing was provided by the Bioinformatics Resource Center (BRC) of the University of Wisconsin-Madison. Fieldwork in Israel was supported by the Israel Taxonomy Initiative (ITI) biodiversity survey grant to E.G.-R. and Y.L., and ITI and HUJI fellowships to S.A., a National Geographic Society Expeditions Council grant no. NGS-271R-18 to J.A. B.. Our study is supported by the United States-Israel Binational Science Foundation grant no. BSF-2019216 to P.P.S. and E.G.-R. This manuscript was improved by valuable comments from the associate editor Harald Letsch, and from M. Pavlek and two anonymous reviewers.

Appendix A. Supplementary material

Supplementary data to this article can be found online at https://doi.org/10.1016/j.ympev.2023.107705.

References

Aharon, S., Ballesteros, J.A., Crawford, A.R., Friske, K., Gainett, G., Langford, B., Santibáñez-López, C.E., Ya'aran, S., Gavish-Regev, E., Sharma, P.P., 2019. The anatomy of an unstable node: a Levantine relict precipitates phylogenomic dissolution of higher-level relationships of the armoured harvestmen (Arachnida: Opiliones: Laniatores). Invert. Systematics. Doi: 10.1071/IS19002.

Arnedo, M.A., Oromí, P., Múrria, C., Macías-Hernández, N., Ribera, C., 2007. The dark side of an island radiation: systematics and evolution of troglobitic spiders of the genus *Dysdera* Latreille (Araneae: Dysderidae) in the Canary Islands. Invertebr. Syst. 21, 623–660.

Baker, C.M., Ballesteros, J.A., Aharon, S., Gainett, G., Armiach Steinpress, I., Wizen, G., Sharma, P.P., Gavish-Regev, E., 2022. Recent speciation and phenotypic plasticity within a parthenogenetic lineage of levantine whip spiders (Chelicerata: Amblypygi: Charinidae). Mol. Phylogenet. Evol. 175, 107560 https://doi.org/10.1016/j.ympev.2022.107560.

Bar-Matthews, M., Ayalon, A., Kaufman, A., Wasserburg, G.J., 1999. The Eastern Mediterranean paleoclimate as a reflection of regional events: Soreq cave, Israel. Earth Planet. Sci. Lett. 166, 85–95.

Barr, T.C., Holsinger, J.R., 1985. Speciation in Cave Faunas. Annu. Rev. Ecol. Syst. 16, 313–337. https://doi.org/10.1146/annurev.es.16.110185.001525.

Bidegaray-Batista, L., Arnedo, M.A., 2011. Gone with the plate: the opening of the Western Mediterranean basin drove the diversification of ground-dweller spiders. BMC Evol Biol 11, 317. https://doi.org/10.1186/1471-2148-11-317.

Biton, R., Boistel, R., Rabinovich, R., Gafny, S., Brumfeld, V., Bailon, S., 2016. Osteological Observations on the Alytid Anura *Latonia nigriventer* with Comments on Functional Morphology, Biogeography, and Evolutionary History: OSTEOLOGY OF LATONIA NIGRIVENTER. J. Morphol. 277, 1131–1145. https://doi.org/10.1002/jmor.20562.

Bolnick, D.I., Fitzpatrick, B.M., 2007. Sympatric Speciation: Models and Empirical Evidence. Annu. Rev. Ecol. Evol. Syst. 38, 459–487. https://doi.org/10.1146/annurev.ecolsys.38.091206.095804.

Bolzern, A., Burckhardt, D., Hänggi, A., 2013. Phylogeny and taxonomy of European funnel-web spiders of the *Tegenaria*–*Malthonica* complex (Araneae: Agelenidae) based upon morphological and molecular data: The *Tegenaria-Malthonica* complex. Zool J Linn Soc 168, 723–848. https://doi.org/10.1111/zoj.12040.

Bouckaert, R., Vaughan, T.G., Barido-Sottani, J., Duchêne, S., Fourment, M., Gavryushkina, A., Heled, J., Jones, G., Kühnert, D., De Maio, N., Matschiner, M., Mendes, F.K., Müller, N.F., Ogilvie, H.A., du Plessis, L., Popinga, A., Rambaut, A., Rasmussen, D., Siveroni, I., Suchard, M.A., Wu, C.-H., Xie, D., Zhang, C., Stadler, T., Drummond, A.J., 2019. BEAST 2.5: An advanced software platform for Bayesian evolutionary analysis. PLoS Comput Biol 15, e1006650.

Bradic, M., Beerli, P., García-de León, F.J., Esquivel-Bobadilla, S., Borowsky, R.L., 2012. Gene flow and population structure in the Mexican blind cavefish complex (*Astyanax mexicanus*). BMC Evol Biol 12, 9. https://doi.org/10.1186/1471-2148-12-9.

Capella-Gutierrez, S., Silla-Martinez, J.M., Gabaldon, T., 2009. trimAl: a tool for automated alignment trimming in large-scale phylogenetic analyses. Bioinformatics 25, 1972–1973. https://doi.org/10.1093/bioinformatics/btp348.

Cuff, J.P., Aharon, S., Armiach Steinpress, I., Seifan, M., Lubin, Y., Gavish-Regev, E., 2021. It's All about the Zone: Spider Assemblages in Different Ecological Zones of Levantine Caves. Diversity 13, 576. https://doi.org/10.3390/d13110576.

Danin, A., 1999. Desert Rocks as Plant Refugia in the near East. Bot. Rev. 65, 93–170.

Derkarabetian, S., Steinmann, D.B., Hedin, M., 2010. Repeated and Time-Correlated Morphological Convergence in Cave-Dwelling Harvestmen (Opiliones, Laniatores) from Montane Western North America. PLoS One 5, e10388.

Dimitrov, D., 2020. Description of a new *Tegenaria* Latreille, 1804 from southern Turkey with remarks on the *Tegenaria ariadnae* species-complex (Arachnida, Araneae). ZK 935, 47–55. https://doi.org/10.3897/zookeys.935.52089.

Dimitrov, D., Bolzern, A., Arnedo, M., 2022. Bringing *Tegenaria boitanii* stat. rev. back to life with a review of the *Tegenaria percuriosa* -complex (Araneae: Agelenidae), description of a new species and insight into their phylogenetic relationships and evolutionary history. Syst. Biodivers. 20, 1–18. https://doi.org/10.1080/14772000.2021.2012297.

Dubey, S., Cosson, J.-F., Magnanou, E., Vohralík, V., Benda, P., Frynta, D., Hutterer, R., Vogel, V., Vogel, P., 2007. Mediterranean populations of the lesser white-toothed shrew (*Crocidura suaveolens* group): an unexpected puzzle of Pleistocene survivors and prehistoric introductions. Mol Ecol 16, 3438–3452. https://doi.org/10.1111/j.1365-294X.2007.03396.x.

Eaton, D.A.R., Overcast, I., 2020. ipyrad: Interactive assembly and analysis of RADseq datasets. Bioinformatics 36, 2592–2594. https://doi.org/10.1093/bioinformatics/btz966.

Elshire, R.J., Glaubitz, J.C., Sun, Q., Poland, J.A., Kawamoto, K., Buckler, E.S., Mitchell, S.E., 2011. A Robust, Simple Genotyping-by-Sequencing (GBS) Approach for High Diversity Species. PLoS One 6, e19379.

Frumkin, A., 1993. Karst origin of the upper erosion surface in the Northern Judean Mountains, Israel. Isr. J. Earth Sci. 41, 169–176.

Frumkin, A., Bar-Matthews, M., Davidovich, U., Langford, B., Porat, R., Ullman, M., Zissu, B., 2014. In-situ dating of ancient quarries and the source of flowstone ('calcite-alabaster') artifacts in the southern Levant. J. Archaeol. Sci. 41, 749–758. https://doi.org/10.1016/j.jas.2013.09.025.

Frumkin, A., Aharon, S., Davidovich, U., Langford, B., Negev, Y., Ullman, M., Vaks, A., Ya'aran, S., Zissu, B.,, 2018. Old and recent processes in a warm and humid desert hypogene cave: 'A'rak Na'asane, Israel. IJS 47, 307–321. https://doi.org/10.5038/1827-806X.47.3.2178.

Frumkin, A., Dimentman, C., Naaman, I., 2020. Biogeography of living fossils as a key for geological reconstruction of the East Mediterranean: Ayyalon - Nesher Ramla system Israel. Quat. Int. S104061822030803X https://doi.org/10.1016/j.quaint.2020.11.036.

Frumkin, A., Ben-Tov, D., Buslov, V., Langford, B., Valdman, E., Yaaran, S., 2017. The southernmost authigenic karst plateau of the Levant. Proceedings of the 17th International Congress of Speleology Sydney 2, 13–16.

Frumkin, A., Fischhendler, I., 2005. Morphometry and distribution of isolated caves as a guide for phreatic and confined paleohydrological conditions. Geomorphology 67, 457–471.

Gavish-Regev, E., Aharon, S., Armiach, I., Lubin, Y., 2016. Cave survey yields a new spider family record for Israel. aramit 51, 39–42. https://doi.org/10.5431/aramit5105.

Gavish-Regev, E., Aharon, S., Armiach Steinpress, I., Seifan, M., Lubin, Y., 2021. A Primer on Spider Assemblages in Levantine Caves: The Neglected Subterranean Habitats of the Levant—A Biodiversity Mine. Diversity 13, 179. https://doi.org/10.3390/d13050179.

Gavrilets, S., 2003. Perspective: models of speciation: what have we learned in 40 years? Evolution 57, 2197–2215. https://doi.org/10.1111/j.0014-3820.2003.tb00233.x.

Gavrilets, S., 2014. Models of Speciation: Where Are We Now? J. Hered. 105, 743–755. https://doi.org/10.1093/jhered/esu045.

Griswold, C., Audisio, T., Ledford, J., 2012. An extraordinary new family of spiders from caves in the Pacific Northwest (Araneae, Trogloraptoridae, new family). ZK 215, 77–102. https://doi.org/10.3897/zookeys.215.3547.

Hoang, D.T., Chernomor, O., von Haeseler, A., Minh, B.Q., Vinh, L.S., 2018. UFBoot2: Improving the Ultrafast Bootstrap Approximation. Mol. Biol. Evol. 35, 518–522. https://doi.org/10.1093/molbev/msx281.

Howarth, F.G., 1980. The Zoogeography Of Specialized Cave Animals: A Bioclimatic Model. Evolution 34, 394–406. https://doi.org/10.1111/j.1558-5646.1980.tb04827.x.

Howarth, F., 1987. The evolution of non-relictual tropical troglobites. IJS 16, 1–16. https://doi.org/10.5038/1827-806X.16.1.1.

Howarth, F.G., 1993. High-Stress Subterranean Habitats and Evolutionary Change in Cave-Inhabiting Arthropods. Am. Nat. 142, S65–S77. https://doi.org/10.1086/285523.

Howarth, F.G., Moldovan, O.T., 2018. The Ecological Classification of Cave Animals and Their Adaptations, in: Moldovan, O.T., Kováč, Ľ., Halse, S. (Eds.), Cave Ecology, Ecological Studies. Springer International Publishing, Cham, pp. 41–67. Doi: 10.1007/978-3-319-98852-8_4.

Howarth, F.G., 2019. Adaptive shifts, in: Encyclopedia of Caves. Elsevier, pp. 47–55. Doi: 10.1016/B978-0-12-814124-3.00007-8.

Juan, C., Guzik, M.T., Jaume, D., Cooper, S.J.B., 2010. Evolution in caves: Darwin's 'wrecks of ancient life' in the molecular era. Mol. Ecol. 19, 3865–3880. https://doi.org/10.1111/j.1365-294X.2010.04759.x.

Kalyaanamoorthy, S., Minh, B.Q., Wong, T.K.F., von Haeseler, A., Jermiin, L.S., 2017. ModelFinder: fast model selection for accurate phylogenetic estimates. Nat. Methods 14, 587–589. https://doi.org/10.1038/nmeth.4285.

Katoh, K., Standley, D.M., 2013. MAFFT Multiple Sequence Alignment Software Version 7: Improvements in Performance and Usability. Mol. Biol. Evol. 30, 772–780. https://doi.org/10.1093/molbev/mst010.

Langford, B., Frumkin, A., Valdman, E., Ya'aran, S., Buslov, V., Lisovich, Y.,, 2019. The Epigenic Karst field of Ofra, the southernmost Holokarst region in the Levant. Studies on the Land of Judea: Proceedings of the 3rd Annual Conference in Memory of Dr. David Amit 265–280.

Lecigne, S., 2021. A new species of *Sintula* (Linyphiidae), redescription of *Brigittea innocens* (Dictynidae) and eight spider species newly recorded for Turkey (Araneae). Arachnol. Mitteilungen: Arachnol. Lett. 62 https://doi.org/10.30963/aramit6204.

Levy, G., 1996. The agelenid funnel-weaver family and the spider genus *Cedicus* in Israel (Araneae, Agelenidae and Cybaeidae). Zool. Scr. 25, 85–122.
Magalhaes, I.L.F., 2019. Spreadsheets to expedite taxonomic publications by automatic generation of morphological descriptions and specimen lists. Zootaxa 4624, 147–150. https://doi.org/10.11646/zootaxa.4624.1.12.
Mammola, S., 2019. Finding answers in the dark: caves as models in ecology fifty years after Poulson and White. Ecography 42, 1331–1351. https://doi.org/10.1111/ecog.03905.
Mammola, S., Isaia, M., Arnedo, M.A., 2015. Alpine endemic spiders shed light on the origin and evolution of subterranean species. PeerJ 3, e1384.
Mammola, S., Arnedo, M.A., Pantini, P., Piano, E., Chiappetta, N., Isaia, M., 2018. Ecological speciation in darkness? Spatial niche partitioning in sibling subterranean spiders (Araneae : Linyphiidae : *Troglohyphantes*). Invert. Systematics 32, 1069. https://doi.org/10.1071/IS17090.
Mammola, S., Pavlek, M., Huber, B.A., Isaia, M., Ballarin, F., Tolve, M., Čupić, I., Hesselberg, T., Lunghi, E., Mouron, S., Graco-Roza, C., Cardoso, P., 2022a. A trait database and updated checklist for European subterranean spiders. Sci. Data 9, 236. https://doi.org/10.1038/s41597-022-01316-3.
Mammola, S., Pavlek, M., Huber, B.A., Isaia, M., Ballarin, F., Tolve, M., Čupić, I., Hesselberg, T., Lunghi, E., Mouron, S., Roza, C.G., Cardoso, P., 2022b. A trait database for European subterranean spiders. https://doi.org/10.6084/M9.FIGSHARE.16574255.
Nguyen, L.-T., Schmidt, H.A., von Haeseler, A., Minh, B.Q., 2015. IQ-TREE: A Fast and Effective Stochastic Algorithm for Estimating Maximum-Likelihood Phylogenies. Mol. Biol. Evol. 32, 268–274. https://doi.org/10.1093/molbev/msu300.
Peterson, B.K., Weber, J.N., Kay, E.H., Fisher, H.S., Hoekstra, H.E., 2012. Double Digest RADseq: An Inexpensive Method for De Novo SNP Discovery and Genotyping in Model and Non-Model Species. PLoS One 7, e37135.
Poulson, T.L., White, W.B., 1969. The Cave Environment. Science 165, 971–981. https://doi.org/10.1126/science.165.3897.971.
Protas, M., Jeffery, W.R., 2012. Evolution and development in cave animals: from fish to crustaceans: Evolution and development in cave animals. WIREs Dev Biol 1, 823–845. https://doi.org/10.1002/wdev.61.
Rambaut, A., Drummond, A.J., Xie, D., Baele, G., Suchard, M.A., 2018. Posterior Summarization in Bayesian Phylogenetics Using Tracer 1.7. Syst. Biol. 67, 901–904. https://doi.org/10.1093/sysbio/syy032.
Reznick, D.N., Ricklefs, R.E., 2009. Darwin's bridge between microevolution and macroevolution. Nature 457, 837–842. https://doi.org/10.1038/nature07894.
Rivera, M.A.J., Howarth, F.G., Taiti, S., Roderick, G.K., 2002. Evolution in Hawaiian cave-adapted isopods (Oniscidea: Philosciidae): vicariant speciation or adaptive shifts? Mol. Phylogenet. Evol. 25, 1–9. https://doi.org/10.1016/S1055-7903(02)00353-6.
Romero Díaz, A., Fenolio, D., 2009. Cave biology: life in darkness, Ecology, biodiversity, and conservation. Cambridge Univ. Press, Cambridge.
Rundle, H.D., Nosil, P., 2005. Ecological speciation: Ecological speciation. Ecol. Lett. 8, 336–352. https://doi.org/10.1111/j.1461-0248.2004.00715.x.
Savolainen, V., Anstett, M.-C., Lexer, C., Hutton, I., Clarkson, J.J., Norup, M.V., Powell, M.P., Springate, D., Salamin, N., Baker, W.J., 2006. Sympatric speciation in palms on an oceanic island. Nature 441, 210–213. https://doi.org/10.1038/nature04566.
Schluter, D., 2009. Evidence for Ecological Speciation and Its Alternative. Science 323, 737–741. https://doi.org/10.1126/science.1160006.
Shahack-Gross, R., Berna, F., Karkanas, P., Weiner, S., 2004. Bat guano and preservation of archaeological remains in cave sites. J. Archaeol. Sci. 31, 1259–1272. https://doi.org/10.1016/j.jas.2004.02.004.
Snowman, C.V., Zigler, K.S., Hedin, M., 2010. Caves as islands: mitochondrial phylogeography of the cave-obligate spider species *Nesticus barri* (Araneae: Nesticidae). The Journal of Arachnology 38, 49–56.
Strecker, U., Bernatchez, L., Wilkens, H., 2003. Genetic divergence between cave and surface populations of *Astyanax* in Mexico (Characidae, Teleostei). Mol. Ecol. 12, 699–710. https://doi.org/10.1046/j.1365-294X.2003.01753.x.
Tchernov, E., 1988. The biogeographical history of the southern Levant., in: The Zoogeography of Israel. The Distribution and Abundance at a Zoogeographical Crossroad. pp. 159–250.
Tobin, B.W., Hutchins, B.T., Schwartz, B.F., 2013. Spatial and temporal changes in invertebrate assemblage structure from the entrance to deep-cave zone of a temperate marble cave. Int. J. Speleobiol. 42, 203–221. https://doi.org/10.5038/1827-806X.42.3.
Toft, S., Lubin, Y., 2018. The egg sac of *Benoitia lepida* (Araneae: Agelenidae): structure, placement and the function of its layers. J. Arachnol. 46, 35–39. https://doi.org/10.1636/JoA-S-17-020.1.
Trajano, E., de Carvalho, M.R., 2017. Towards a biologically meaningful classification of subterranean organisms: a critical analysis of the Schiner-Racovitza system from a historical perspective, difficulties of its application and implications for conservation. SB 22, 1–26. https://doi.org/10.3897/subtbiol.22.9759.
Trajano, E., 2012. Ecological Classification of Subterranean Organisms, in: Encyclopedia of Caves. Elsevier, pp. 275–277. Doi: 10.1016/B978-0-12-383832-2.00035-9.
Trontelj, P., 2018. Structure and Genetics of Cave Populations. In: Moldovan, O.T., Kováč, Ľ., Halse, S. (Eds.), Cave Ecology, Ecological Studies. Springer International Publishing, Cham, pp. 269–295. https://doi.org/10.1007/978-3-319-98852-8_12.
Turelli, M., Barton, N.H., Coyne, J.A., 2001. Theory and speciation. Trends Ecol. Evol. 16, 330–343. https://doi.org/10.1016/S0169-5347(01)02177-2.
Turk, S., Sket, B., Sarbu, Ş., 1996. Comparison between some epigean and hypogean populations of *Asellus aquaticus* (Crustacea: Isopoda: Asellidae). Hydrobiologia 337, 161–170. https://doi.org/10.1007/BF00028517.
World Spider Catalog Version 23.5 [WWW Document], 2022. URL http://wsc.nmbe.ch (accessed 11.7.22).
Yechezkel, A., Frumkin, A., 2016. Spring tunnels (Niqba'): The Jerusalem hills perspective. Underground aqueducts handbook.
Zissu, B., Klein, E., Davidovich, U., Porat, R., Langford, B., Frumkin, A., 2011a. A Pagan Cult Site (?) from the Late Roman Period in the Te'omim Cave, Western Jerusalem Hills. New Stud. Jerusalem 17, 311–341.
Zissu, B., Porat, R., Langford, B., Frumkin, A., 2011b. Archaeological remains of the Bar Kokhba Revolt in the Tẻomim Cave (Mūghâret Umm et Tûeimîn), Western Jerusalem Hills. JJS 62, 262–283. https://doi.org/10.18647/3043/JJS-2011.
Zohary, M., 1962. Plant Life of Palestine. The Ronald Press, New York, Israel and Jordan.